

Award Number: W81XWH-04-1-0149

TITLE: The Role of the Caspase-8 Inhibitor FLIP in Androgen-Withdrawal Induced Death of Prostate Epithelium

PRINCIPAL INVESTIGATOR: John Krolewski, M.D., Ph.D.
Kent Nastiuk, Ph.D.

CONTRACTING ORGANIZATION: University of California
Irvine, CA 92679

REPORT DATE: January 2006

TYPE OF REPORT: Annual

PREPARED FOR: U.S. Army Medical Research and Materiel Command
Fort Detrick, Maryland 21702-5012

DISTRIBUTION STATEMENT: Approved for Public Release;
Distribution Unlimited

The views, opinions and/or findings contained in this report are those of the author(s) and should not be construed as an official Department of the Army position, policy or decision unless so designated by other documentation.

REPORT DOCUMENTATION PAGEForm Approved
OMB No. 0704-0188

Public reporting burden for this collection of information is estimated to average 1 hour per response, including the time for reviewing instructions, searching existing data sources, gathering and maintaining the data needed, and completing and reviewing this collection of information. Send comments regarding this burden estimate or any other aspect of this collection of information, including suggestions for reducing this burden to Department of Defense, Washington Headquarters Services, Directorate for Information Operations and Reports (0704-0188), 1215 Jefferson Davis Highway, Suite 1204, Arlington, VA 22202-4302. Respondents should be aware that notwithstanding any other provision of law, no person shall be subject to any penalty for failing to comply with a collection of information if it does not display a currently valid OMB control number. **PLEASE DO NOT RETURN YOUR FORM TO THE ABOVE ADDRESS.**

1. REPORT DATE 01-01-2006		2. REPORT TYPE Annual		3. DATES COVERED 1 Jan 2005 – 30 Dec 2005	
4. TITLE AND SUBTITLE The Role of the Caspase-8 Inhibitor FLIP in Androgen-Withdrawal Induced Death of Prostate Epithelium				5a. CONTRACT NUMBER	
				5b. GRANT NUMBER W81XWH-04-1-0149	
				5c. PROGRAM ELEMENT NUMBER	
6. AUTHOR(S) John Krolewski, M.D., Ph.D. Kent Nastiuk, Ph.D.				5d. PROJECT NUMBER	
				5e. TASK NUMBER	
				5f. WORK UNIT NUMBER	
7. PERFORMING ORGANIZATION NAME(S) AND ADDRESS(ES) University of California Irvine, CA 92679				8. PERFORMING ORGANIZATION REPORT NUMBER	
9. SPONSORING / MONITORING AGENCY NAME(S) AND ADDRESS(ES) U.S. Army Medical Research and Materiel Command Fort Detrick, Maryland 21702-5012				10. SPONSOR/MONITOR'S ACRONYM(S)	
				11. SPONSOR/MONITOR'S REPORT NUMBER(S)	
12. DISTRIBUTION / AVAILABILITY STATEMENT Approved for Public Release; Distribution Unlimited					
13. SUPPLEMENTARY NOTES Original contains colored plates ALL DTIC reproductions will be in black and white					
14. ABSTRACT Secretory prostatic epithelial cells undergo apoptosis in response to androgen deprivation. Similarly, metastatic prostate cancers, which resemble secretory epithelium, also undergo apoptosis following androgen deprivation. Recent evidence suggests that death receptor signaling is required for prostate epithelial cell death following androgen withdrawal. We sought to extend this observation by investigating the role of death receptor signaling components in models of prostate epithelial cell death. Preliminary experiments suggest that FLIP can inhibit apoptosis of prostate epithelial cells. FLIP is an enzymatically inactive version of pro-caspase-8 which negatively regulates cell death, apparently via a dominant-negative mechanism. Based on our preliminary data, we hypothesize that FLIP is a key regulator of prostate apoptosis in response to androgen withdrawal. To address our hypothesis we propose a systematic approach involving, sequentially, correlative (aim 1), functional (aim 2) and mechanistic (aims 3 and 4) experiments. The specific aims are: i) correlate the pattern of FLIP expression with prostate epithelial cell death; ii) assess the functional consequences of forced FLIP expression on prostate epithelial apoptosis; iii) determine which death receptor pathway is involved in prostate epithelial cell death and iv) determine if androgens regulate the level of FLIP expression at the level of gene transcription.					
15. SUBJECT TERMS Prostate Cancer					
16. SECURITY CLASSIFICATION OF:			17. LIMITATION OF ABSTRACT	18. NUMBER OF PAGES	19a. NAME OF RESPONSIBLE PERSON USAMRMC
a. REPORT U	b. ABSTRACT U	c. THIS PAGE U			19b. TELEPHONE NUMBER (include area code)
			UU	53	

Table of Contents

Cover.....	1
SF 298.....	2
Introduction.....	4
Body.....	4
Key Research Accomplishments.....	6
Reportable Outcomes.....	6
Conclusions.....	7
References.....	None
Appendices.....	8

INTRODUCTION: Our long term goal is to identify the molecular events which trigger androgen withdrawal induced apoptosis (AWIA), in order to discover novel targets for prostate cancer therapy. The studies focus on FLIP, an inactive homologue of caspase-8, which inhibits apoptosis. Based on our preliminary studies, we hypothesize that FLIP plays a key role in AWIA. Specifically, we propose that FLIP protein levels are transcriptionally down-regulated following androgen withdrawal, permitting the activation of one or more death receptor signaling pathways.

PROGRESS REPORT:

Task 1. Correlate the decline in FLIP expression with the onset of prostate epithelial cell death (months 1-6).

- 1.1 Employ affinity precipitation and immunoblotting to measure FLIP protein levels in apoptosing rat prostate glands.
- 1.2 Use immunohistochemistry and *in situ* hybridization to determine the spatial (cell-type specific) pattern of FLIP expression in apoptosing rat prostate glands.
- 1.3 Measure the levels of FLIP mRNA (by quantitative RT-PCR) and protein (by affinity precipitation and immunoblotting) in NRP-152 cells induced to apoptose by TGF β .

Results: We previously reported having found that FLIP protein levels decline by 24 hours post-castration, before the onset of AWIA in the prostates of castrated rats (task 1.1). This data is shown in Fig. 1 in the Appendix. We expect that FLIP mRNA and protein levels will be mainly modulated in apoptosing secretory epithelium, rather than in apoptosis-resistant basal epithelial and stromal cells, but have not yet undertaken the studies to confirm this (task 1.2). Since differentiation sensitizes NRP-152 cells to TGF β killing, our hypothesis suggests that both FLIP mRNA and protein levels should decline in terminally differentiated NRP-152 cells. Indeed, immunoblots of NRP-152 cells undergoing differentiation show a complex regulation, with an initial decline in FLIP protein levels, followed by an increase within 24 hours. TGF β blocks this later increase in FLIP protein levels (task 1.3) (see manuscript Figs. 1 and 7).

Task 2. Assess the functional consequences of forced FLIP expression on prostate epithelial apoptosis (months 1-36).

- 2.1 Create NRP-152 cells expressing an inducible FLIP transgene and confirm our preliminary observation that FLIP overexpression inhibits TGF β induced apoptosis of this immortalized prostate epithelial cell line.
- 2.2 Generate an adenovirus expressing FLIP-IRES-GFP, infect rat prostate glands and determine if constitutive FLIP over-expression inhibits castration induced prostate epithelial cell death.
- 2.3 Create inducible FLIP transgenic mice and determine if FLIP over-expression inhibits castration induced prostate epithelial cell death.

Results: Inducible expression constructs in NRP-152 cells have proven unsuitable due to the loss of TGF β responsiveness during selection of the ecdysone inducible clones.

We therefore isolated additional constitutively expressing FLIP short NRP clones to extend our analysis (see manuscript Fig 4). Forced expression of FLIP short inhibits TGF β induced cell death in NRP-152 cells and the inhibition is dependent on the level of FLIP expression. Clones expressing FLIP short fail to show the increased caspase activity that accompanies TGF β treatment of control NRP-152 cells (task 2.1) (see manuscript Figs. 1, 3 and 4). Additionally, we have begun a new round of isolation of tetracycline-inducible NRP-152 clones in order to revisit whether acute modulation of FLIP, as well as modulators of FLIP regulators, affect prostate cell survival. Adenoviruses expressing GFP alone and both the long and short forms of FLIP with an IRES-driven GFP cassette have been produced (see Figure 2). Unfortunately, the FLIP long expressing adenovirus does not infect either rat or human prostate cells in culture (data not shown). The FLIP short adenovirus does infect NRP-152 (and other) prostate cell lines, but induces apoptosis at high MOI (Figure 3A). Lowering the MOI reduces the proportion of GFP positive cells, as expected (Figure 3B and C), but at these reduced MOI levels, while there is no increased adenoviral-induced cell death, there is also only partial protection of the NRP-152 cells from TGF β 1-induced cell death. When 50% of the cells are infected (MOI=4), only ~33% of the infected cells die, versus 75% of uninfected cells (Figure 3D, 3E). We are currently assessing better titration of the viral MOI (task 2.2). We have not yet begun creating a mouse line with inducible expression of a FLIP transgene (task 2.3).

Task 3. *Examine the mechanism of FLIP action by determining which death receptor pathway is inhibited by FLIP during prostate epithelial apoptosis (months 24-36).*

- 3.1 Determine if Fas and/or TRAIL KO mice are resistant to, or show a reduction in the extent of, castration induced prostate cell death.
- 3.2 Determine if recombinant death receptor ligands (FasL and TRAIL) induce cell death in NRP-152 cells and primary prostate epithelial cells.

Results: Initial experiments using wild-type mice were technically unsatisfactory due to excessive variability derived from the difficulty in dissecting the prostate lobes from the surrounding tissue. We have therefore been developing an MRI method with a 7 Tesla small animal MRI since it allows us to more precisely make volume measurements of the organ and to follow the same animal over time, as it is non-invasive. Appendix Figs 4-5 summarize our findings, demonstrating the general reproducibility of the MRI measurements in assessing the size of intact prostates (Fig. 5A) and the involution of the prostate and its subsequent re-growth stimulated by androgens as assessed by MRI (Figs. 4 and 5B and 5C). We are now awaiting delivery of TRAIL $-/-$ mice from Amgen according to our agreement with them to assess castration-induced regression in mature male mice. We predict that TRAIL might be the death receptor ligand that mediates apoptosis in prostate epithelium and therefore, we expect TRAIL KO mice will be refractory to AWIA (task 3.1). We have demonstrated that recombinant FasL and TRAIL will induce apoptosis in NRP cells (see manuscript Fig. 5B and 6C, respectively), but while Fas-Fc, DR4-Fc and DR5-Fc block TRAIL-induced death in Jurkat cells (manuscript Figs. 5B, 6A-B), they fail to

block TGF β -induced death in NRP cells (manuscript Figs. 5C-D, 6D-F). While we produced rat Fas-Fc, we used human DR4 and DR5 reagents in these studies. We are therefore producing rat DR5-Fc protein, as we did for the rat Fas-Fc, to rule out the possibility of inter-species variability resulting in the lack of effect of blocking TRAIL signaling in NRP-152 cells reported in the manuscript. We have not yet undertaken similar studies in primary prostate epithelial cells (task 3.2).

Task 4. Characterize androgen regulation of FLIP expression in the androgen-responsive cell line LNCaP.

- 4.1 Use immunoblotting, RT-PCR and reporter gene assays to determine if androgen-mediated regulation of FLIP occurs at the level of gene transcription.

Results: We have observed androgen mediated modulation of FLIP protein in LNCaP cells and predict that the FLIP gene is regulated by androgen at the level of gene transcription (Appendix Fig. 6). We have found that the regulation of FLIP is dependent on the PTEN state of the cells, and that in LNCaP cells, which lack PTEN, the PI3K inhibitor LY294002 is required to see modulation of FLIP protein (Appendix Fig. 7). These effects are also apparent at the mRNA levels of FLIP, but in combination, they neutralize each other (Appendix Fig. 8). We have also observed a role for Akt activators such as insulin in modulating FLIP expression (manuscript Fig. 7). We now find androgen regulation of several reporter constructs driven by portions of the FLIP promoter in LNCaP cells (Appendix Fig. 9), and in addition find an insulin regulated Forkhead transcription factor (FOXO3a) binding site is important in regulating transcription from the FLIP promoter (task 4.1).

KEY RESEARCH ACCOMPLISHMENTS:

- Define the complex regulation of FLIP protein in differentiating NRP cells
- Isolate and characterize additional FLIP short expressing NRP clones
- Production of adenoviruses expressing FLIP short and long with IRES-GFP
- Developed MRI methodology to measure prostate volume changes in the same animal over time.
- Demonstrate importance of AKT signaling in regulating FLIP protein levels
- Demonstrate androgen and FOXO3a regulation of transcription from the human FLIP promoter

REPORTABLE OUTCOMES:

1. Presentation at the UCI Campuswide Cancer Symposium, 5/05
2. Manuscript submitted to Molecular Cancer Research, 8/05
3. Production of two novel adenoviruses, rat FLIP short and long

CONCLUSIONS: We continue to make good progress in overcoming the inherent problems working with normal rodent prostate biology. The shifting phenotype during selection of clones of NRP cells for isolation of inducible FLIP clones made it a less desirable alternative than isolation of additional constitutively expressing clones to characterize TGF β -induce apoptosis. The small size and interdigitated nature of the mouse prostate made characterizing AWIA much less reliable than in the rat. We therefore developed the MRI method, which is more precise than dissecting and weighing, since we are able to sample the same animal over time, rather than the mean of groups of mice sacrificed at different times, and are able to monitor both the regression and androgen stimulated regrowth in the same animal. Regulation of FLIP in the human prostate cancer cell line LNCaP appears to be under control of both androgens and the growth factor signaling pathway involving AKT acting via Foxo3a. We expect that prostate cells with wild-type levels of PTEN will show more consistent regulation of FLIP by androgens.

REFERENCES: None

APPENDIX: See attached table of contents

APPENDIX

Figure 1 FLIP protein levels decline following castration

Figure 2. Production and expression of FLIP expressing Adenovirus.

Figure 3. Adenoviral FLIP short (AdF_{SH}) expression kills NRP-152 cells.

Figure 4. MRI documents involution of mouse prostate following castration.

Figure 5. Quantitation of MRI data.

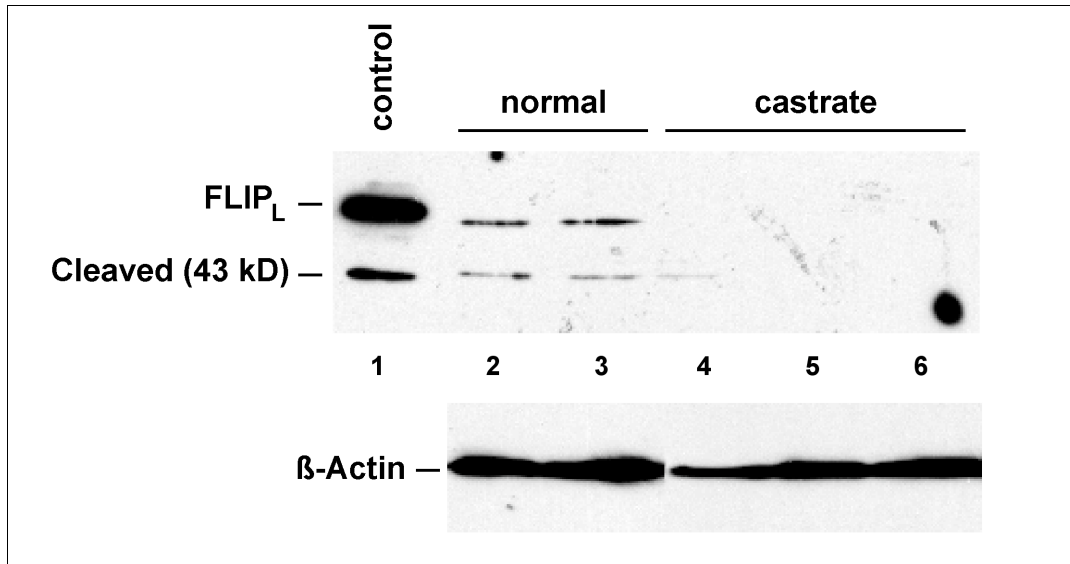
Figure 6. FLIP protein levels decline in response to increasing androgen levels in LNCaP prostate epithelial cells.

Appendix Figure 7. Inhibition of PI3K-Akt activity by LY294002 decreases FLIP protein levels.

Figure 8. AKT and androgens regulate FLIP mRNA.

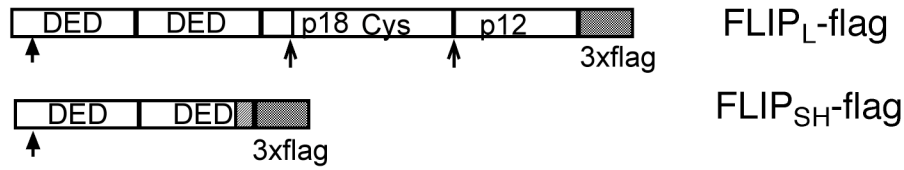
Figure 9. Transcription from the human FLIP promoter is regulated by both LY294002 and androgen treatment.

MANUSCRIPT (submitted to Molecular Cancer Research)

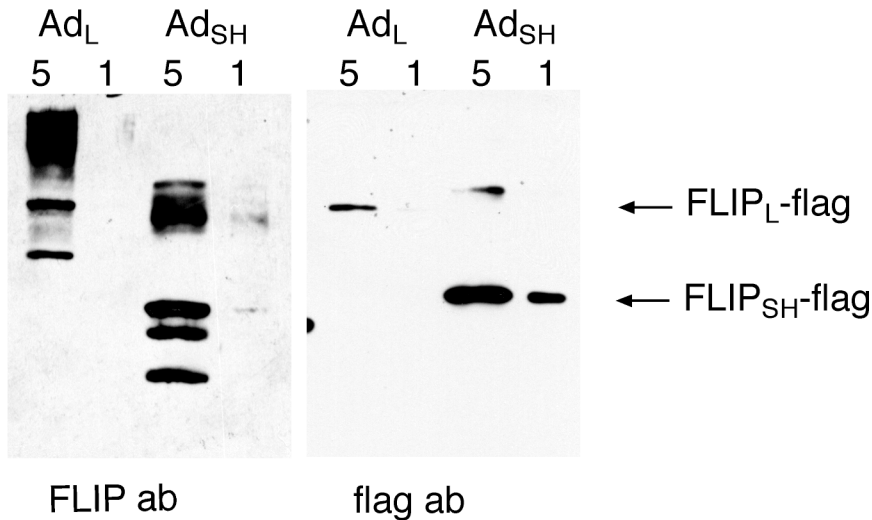


Appendix Figure 1. FLIP protein levels decline following castration. Rats were surgically castrated or sham operated and 24 h later prostate glands were removed and protein lysates prepared. MBP-DED fusion proteins were used to affinity precipitate FLIP proteins (in the presence of z-VAD to prevent caspase activation during purification) and the resulting protein complexes were immunoblotted with an anti-FLIP antibody (upper panels). Extracts were probed with anti-actin to confirm that equal amounts of protein were input to each affinity precipitation reaction. Each lane represents protein recovered from a separate animal (two sham and three castrated animals). As can be seen, the level of FLIP protein declines in the glands from castrated animals, relative to intact animals.

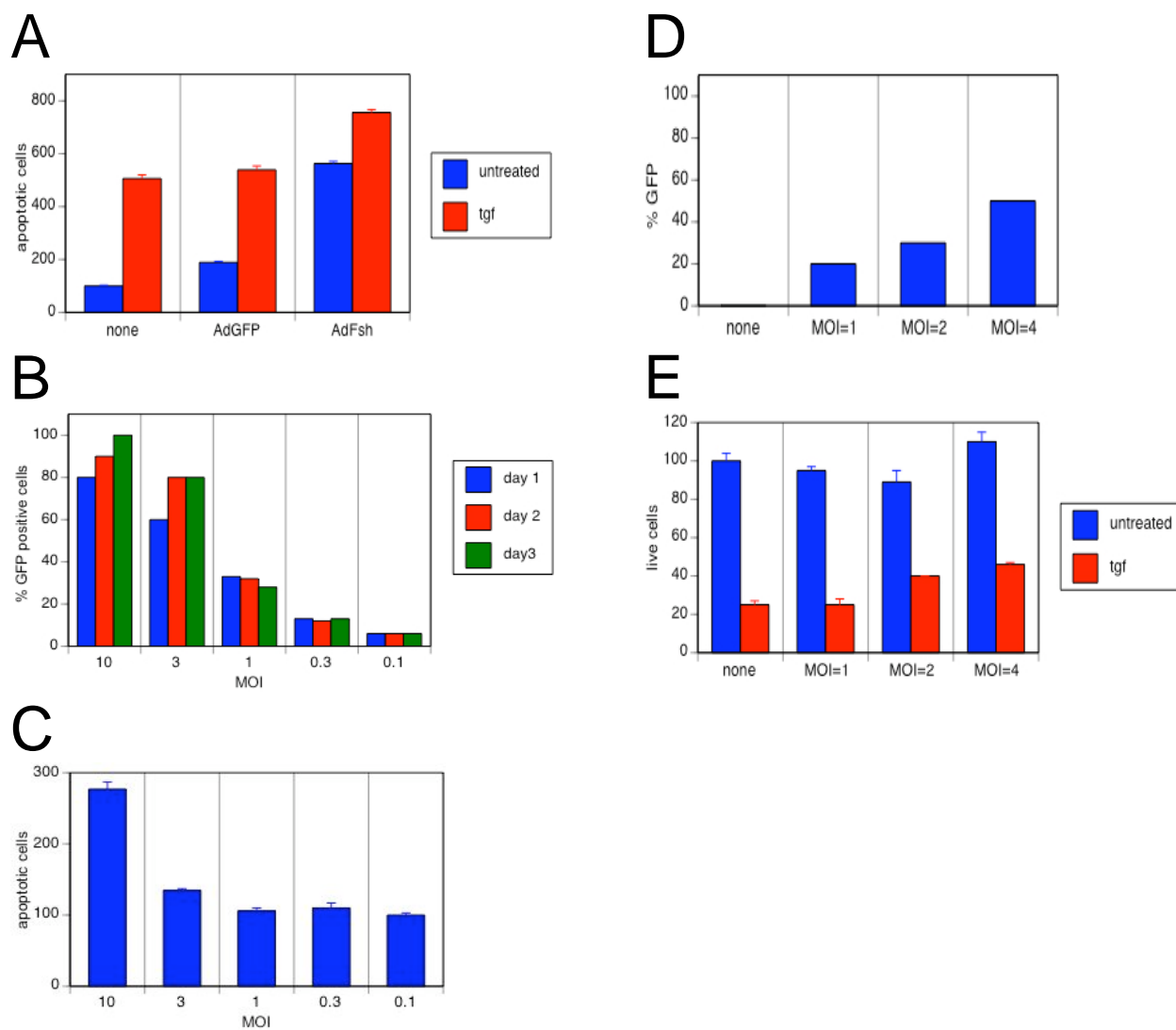
A



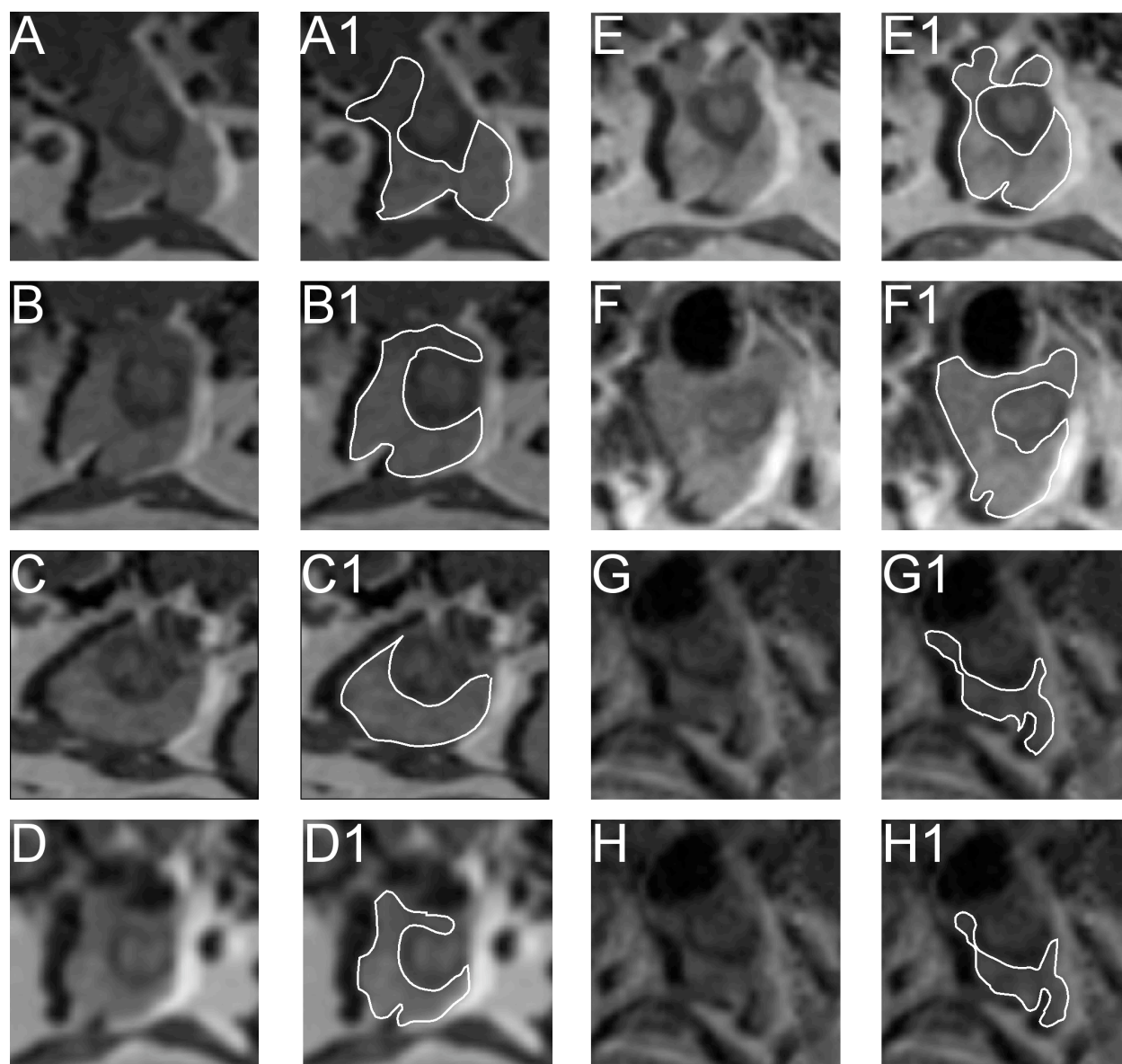
B



Appendix Figure 2. Production and expression of FLIP expressing Adenovirus. A. Diagram of FLIP long (top) and short (bottom) Virus was prepared by flag-tagging the rat cDNAs and inserting them in an adenovirus under control of the CMV promoter and followed by an IRES-GFP cassette. B. 293 cells were infected with either the FLIP long (Ad_L) or short (Ad_{SH}) at the indicated MOI. After 24 hours infection, the cell lysate was examined by SDS-PAGE immunoblotting with either the rat FLIP or flag antibodies (indicated below).

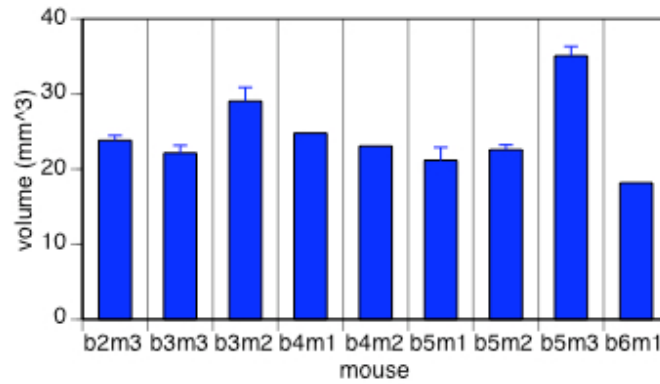


Appendix Figure 3. Adenoviral FLIP short (AdF_{SH}) expression kills NRP-152 cells. A. NRP-152 cells were left uninfected, or infected (MOI=20) with the GFP expressing control virus or FLIP short expressing virus and treated with TGFβ1 for 72 hours. Apoptotic cells as a percentage of the untreated, uninfected control. B, C. Varying the MOI of AdF_{SH} infection of NRP-152 cells from 10 to 0.1 resulted in reduction in the percentage of GFP positive cells and viral-induced apoptosis (as a percentage of the cells infected at MOI=0.1). D, E, F. NRP-152 cells infected with AdF_{SH} at MOI=1 to MOI=4 were partially protected from the apoptosis-inducing effects of TGFβ1. 72 hours after TGF1 addition, live cells were counted and are shown as a percentage of the uninfected, untreated control cell number.

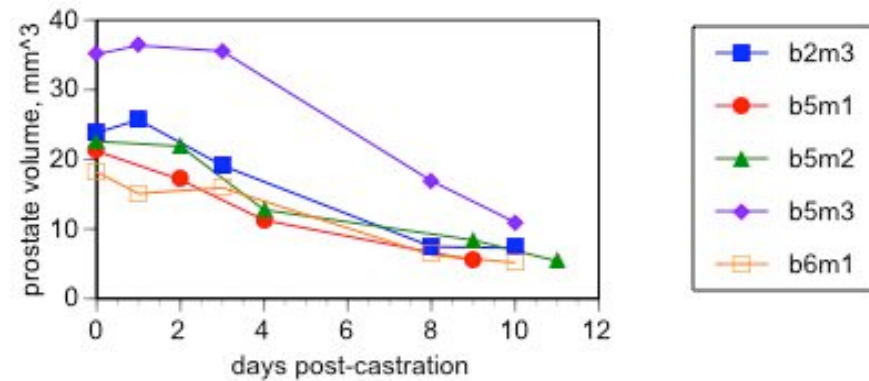


Appendix Figure 4. MRI documents involution of mouse prostate following castration. Adult male mice were either left intact (A-D) or castrated (E-H) and then subjected to imaging via MRI. Panels A-D correspond to four different normal males (A = Batch 3, mouse 2 (b3m2); B = b3m3; C = b4m1; D = b2m3). The corresponding panels A1-D1, show an outline of the ventral lobe of the prostate in one MRI image level. Panels E-H correspond to a single castrated mouse which was imaged at 1, 3, 8 and 10 days post-castration, respectively. The corresponding panels E1-H1, show an outline of the ventral lobe of the prostate in one MRI image level.

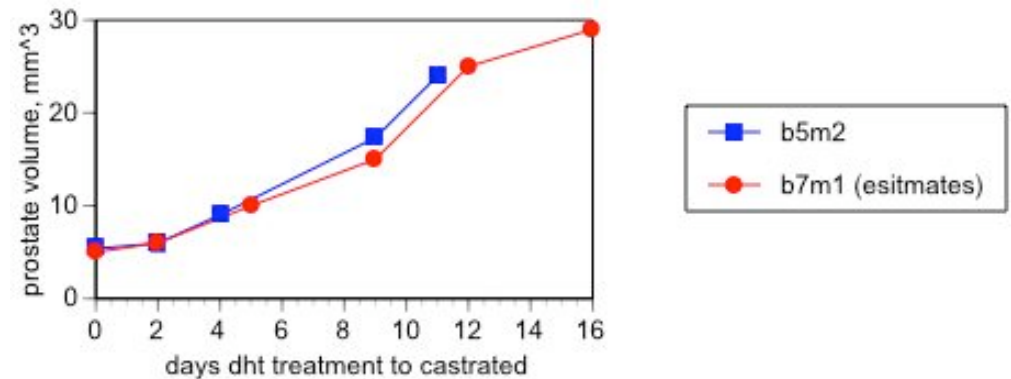
A



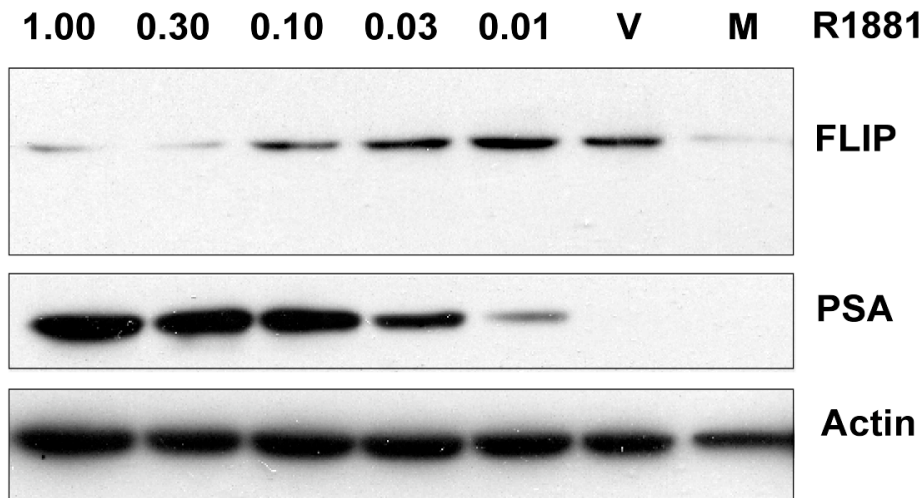
B



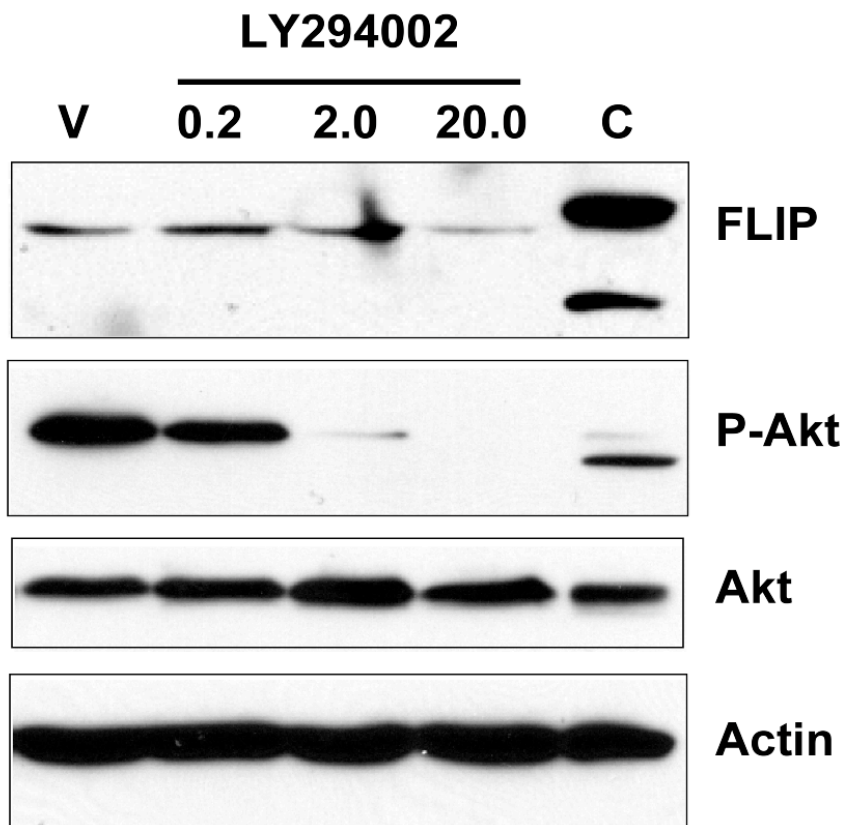
C



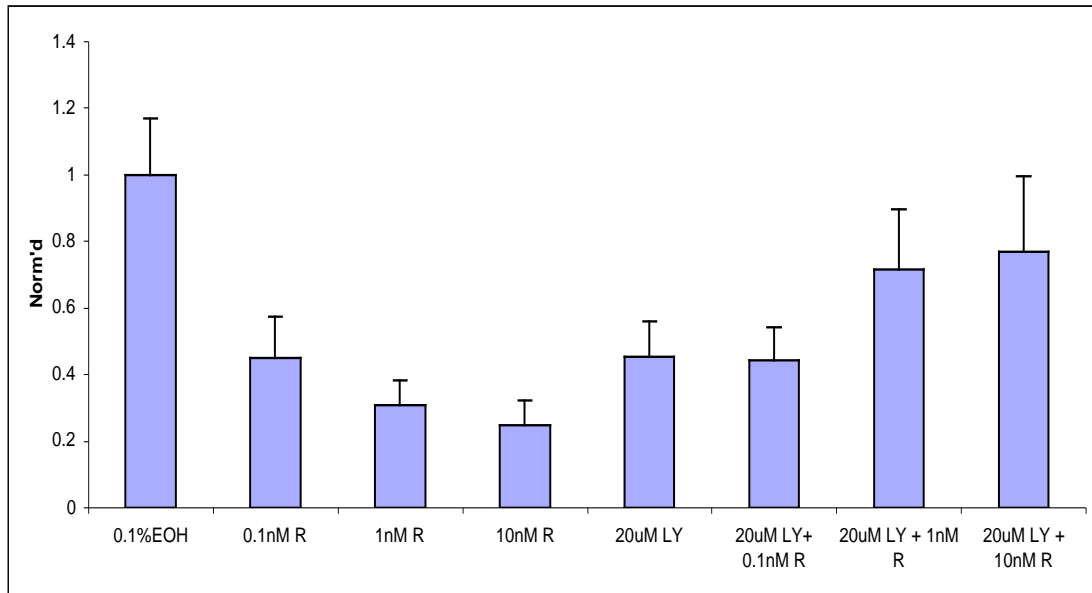
Appendix Figure 5. Quantitation of MRI data. Panel A. MRI determined prostate volumes are reproducible among a cohort of C57/Bl normal mice. Prostate volumes were determined by manually encircling the ventral lobe on each MRI 'slice' and then summing the area of all such slices for a given mouse, examples for four mice are shown in panels A-D of Appendix Figure 4. Note the good reproducibility from animal to animal. Panel B. MRI-derived ventral prostate lobe volume declines post-castration. MRI images were used to calculate ventral prostate volumes as in panel A. These volumes were then plotted as a function of time. As can be seen, there is a clear reduction in the volume of the prostate following castration, which resembles the kinetics of involution observed for the rat prostate (based on weight). Panel C. Two weeks post castration, mice were injected daily with 1mg/kg DHT and the prostate volumes were monitored by MRI imaging, as above. The volume of the prostate returns to pre-castration levels over two weeks, mimicking similar measurements by excision and weighing in rats.



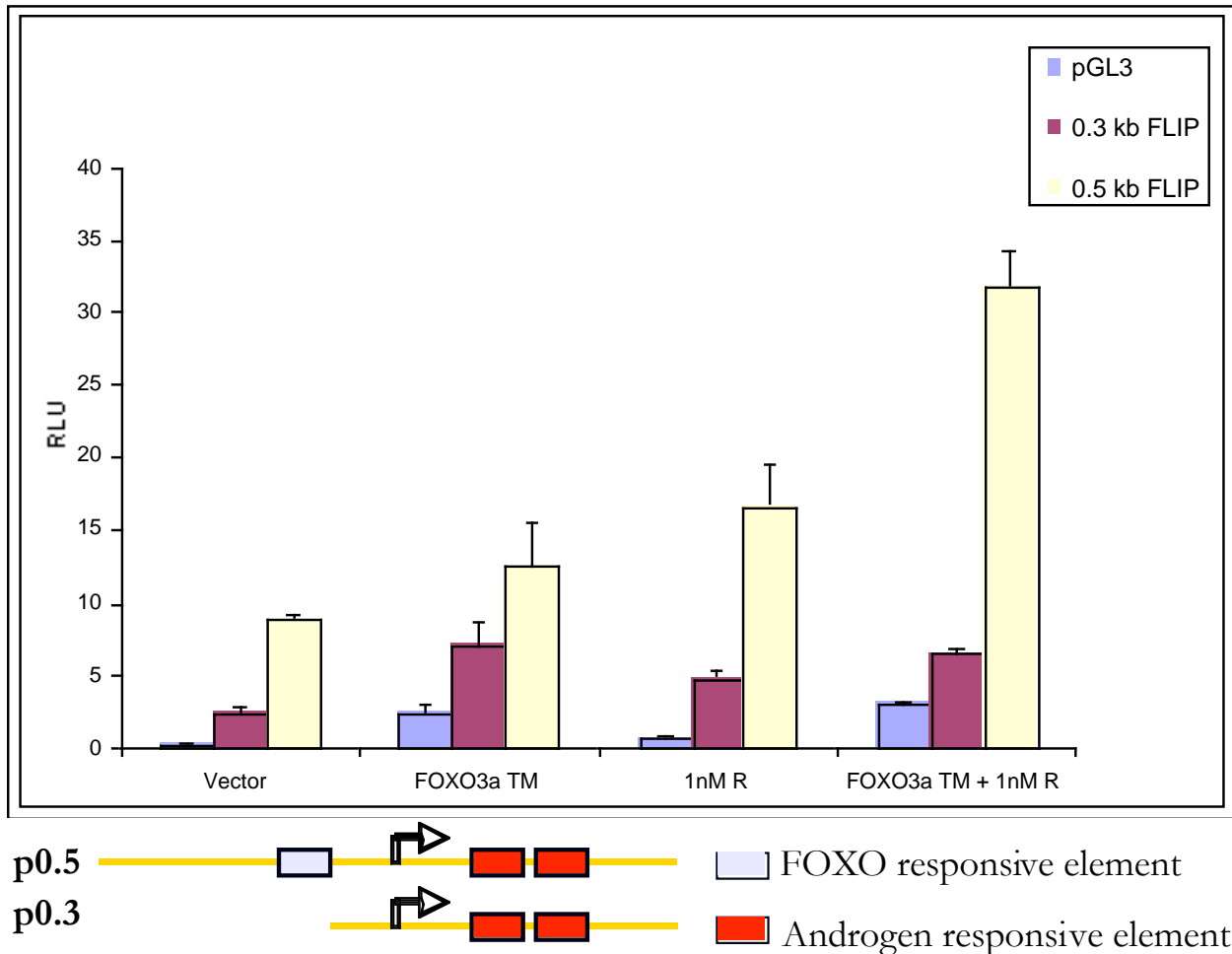
Appendix Figure 6. FLIP protein levels decline in response to increasing androgen levels in LNCaP prostate epithelial cells. LNCaP cells were grown in media with charcoal-stripped serum. Varying amounts of R1881 (as indicated) were added to the cultures and 24 h later post-nuclear supernatant protein extracts were immunoblotted and probed with antibodies against FLIP, PSA and actin (loading control). Lane V corresponds to cells treated with vehicle only. PSA levels indicate the level of androgen response.



Appendix Figure 7. Inhibition of PI3K-Akt activity by LY294002 decreases FLIP protein levels. LNCaP cells were grown in media with charcoal-stripped serum. Varying amounts of LY294002 were added to the cells and 24 h later post-nuclear supernatants protein lysates were prepared and immunoblotted with the indicated antibodies. LNCaP cells are deficient in PTEN and thus have a constitutively active Akt. As shown, increased levels of the inhibitor reduce the level of FLIP protein.



Appendix Figure 8. Inhibition of PI3K-Akt activity by either LY294002 or androgen treatment decreases FLIP mRNA levels but in combination, they increase FLIP mRNA. LNCaP cells were grown in media with charcoal-stripped serum. Varying amounts of R1881 with or without 20 μ M LY294002 were added to the cells and 24 h later total RNA was isolated and reverse transcribed. FLIP mRNA was quantitated relative to actin mRNA. LNCaP cells are deficient in PTEN and thus have a constitutively active Akt. As shown, increased levels of the androgen increased the level of FLIP mRNA in the presence of the AKT inhibitor LY294002.



Appendix Figure 9. Transcription from the human FLIP promoter is regulated by both LY294002 and androgen treatment. LNCaP cells were transfected with the indicated FLIP promoter fragment joined to luciferase, as well as a constitutively active FOXO3a construct (FOXO3a TM) where indicated. R1881 was added to the cells and 24 h later cell lysate was analyzed for luciferase activity. Androgens alone increase transcription, and this is augmented in the presence of the forkhead transcription factor only on the 0.5kb FLIP promoter fragment, but not the 0.3kb fragment which lacks the foxo element.

**FLICE-like inhibitory protein blocks TGFβ1 induced caspase activation
and apoptosis in prostate epithelial cells**

Kent L. Nastiuk¹, Karen Lo¹, Kevin Su¹, Patricia Yeung¹, Julia Kutaka¹, Andrew Cornforth¹,
David Danielpour³ and John J. Krolewski^{*,1,2}

¹Department of Pathology and Laboratory Medicine

²Chao Family Comprehensive Cancer Center

University of California, IRVINE

Irvine, CA 92697, USA

³Division of General Medical Sciences - Oncology

Case Western Reserve University

Cleveland, OH 44106, USA

***Correspondence:**

JJ Krolewski, Department of Pathology and Laboratory Medicine, School of Medicine, UC
Irvine, Medical Sciences I D450, Irvine, CA 92697-4800; E-mail: jkrolews@uci.edu

Phone: 949-824-4089

Running Title: FLIP blocks apoptosis of prostate epithelial cells

Key Words: FLIP, apoptosis, TGFβ, caspase, prostate epithelial cells, NRP-152

Abstract

Androgen withdrawal induces regression of human prostate cancers, but such cancers eventually become androgen independent and metastasize. Thus, deciphering the mechanism of androgen-withdrawal induced apoptosis (AWIA) is critical to designing new therapies for prostate cancer. Previously we demonstrated that in the rat, castration-induced apoptosis is accompanied by a reduction in the expression of the apical caspase inhibitor FLIP (FLICE-like Inhibitory Protein). To test the functional role of FLIP in inhibiting prostate epithelial cell apoptosis, we employed the rat prostate epithelial cell line NRP-152 (NRP). NRP cells differentiate to a secretory phenotype in low-mitogen media and then undergo apoptosis following TGF β 1 addition, mimicking AWIA. NRP cells were stably transfected with constitutively expressed FLIP. NRP clones expressing higher levels of FLIP were refractory to TGF β 1 induced apoptosis. TGF β 1 induced caspase-3 activity is proportional to the level of cell death and inversely proportional to the level of FLIP expression in various clones. Moreover, neither caspase-3 nor PARP is cleaved in clones expressing high level FLIP. To assess whether a death receptor (DR) ligand is involved in TGF β 1 induced apoptosis, we used DR-Fc chimeric proteins that block ligand-receptor interactions. Neither Fas-Fc, DR4-Fc nor DR5-Fc blocked TGF β 1 induced cell death. However, insulin increases FLIP and inhibits NRP death, suggesting that FLIP blocks other DR-ligands and/or mitochondrial apoptosis.

Introduction

Androgens regulate the growth of both normal and neoplastic prostate, and androgen signaling blockade is the primary treatment for late stage prostate cancer. Thus, there is an urgent need to understand the molecular events regulating androgen withdrawal-induced apoptosis (AWIA). As in humans, androgens promote mitosis and differentiation of rodent prostate ductal epithelium, and further, appear to inhibit apoptosis of differentiated cells (1). After androgen ablation in rodents, the balance between mitosis and apoptosis is disrupted, and within two days markers of apoptosis, such as fragmentation of chromosomal DNA, are evident (2, 3). This wave of cell death results in the involution of the prostate gland (4).

A variety of evidence supports the view that TGF β 1 is a paracrine and/or autocrine mediator of AWIA in the intact animal. AWIA is accompanied by an increase in TGF β 1 mRNA, and the kinetics of mRNA induction closely parallel those of AWIA (5). Additionally, there is a concomitant rise in the expression of the RI and RII subunits of the TGF β 1 receptor (6) as well as phosphorylated Smad2, a key downstream mediator of TGF β 1 (4). A dominant negative form of TGF β -RII blocks TGF β 1 induced differentiation and cell death (7, 8). Finally, administration of TGF β 1 to rats results in apoptosis of the prostate (5, 9). Although the mechanism of TGF β 1 action is unclear (it might involve transcriptional effects on pro- and anti-apoptotic proteins (10)), one potential downstream target is the family of death receptor (DR) signaling ligands.

Four extracellular ligands of the TNF family initiate apoptosis through the DRs: TNF, TRAIL, TWEAK, and FasL. The best characterized of these DR ligands is FasL, which signals through the Fas receptor to initiate a cascade of proximal and then distal caspase activation, release of the mitochondrial contents and further caspase activation. This leads to fragmentation of chromosomal DNA, various proteins, and cellular membranes, resulting in cell death (11, 12).

We have previously shown that one inhibitor of the DR pathways, FLICE-like inhibitory protein (FLIP), is down-regulated in the rat prostate following castration (2). FLIP is an inactive homologue of caspase-8, an apical caspase activated in DR signaling. Like caspase-8, FLIP can be recruited to DRs following ligand binding, via the adaptor molecule FADD. Elevated levels of FLIP can displace caspase-8 from the activated DR complex, acting as a dominant inhibitor of caspase-8 and thereby preventing the activation of distal caspases and cell death (13). Surgical specimens from normal human prostate, as well as both androgen responsive and unresponsive tumors, express Fas and FasL (14, 15). TRAIL induced apoptosis can be inhibited by FLIP (16, 17). TRAIL induces apoptosis of both normal prostate epithelial cells (18) and prostate cancer cell lines (19, 20) but many cancers are resistant to TRAIL-induced apoptosis due to over-expression of FLIP. This resistance can be reversed by blocking FLIP expression using chemotherapeutics (21) or siRNA (22-25).

To test the functional role of FLIP in inhibiting prostate epithelial cell apoptosis, we employed the immortalized, non-tumorigenic rat prostate epithelial cell line NRP-152 (NRP) (26). When grown in mitogen-rich media these cells resemble prostate basal epithelia and divide rapidly. In mitogen-poor media, growth is suppressed as the cells differentiate into a secretory phenotype (27). The ability of NRP cells to replicate as basal-like epithelial cells and subsequently differentiate into secretory-like epithelial cells *in vivo* and *in vitro* suggests this cell line is an excellent model for normal prostatic epithelium. It is the secretory epithelium of the prostate which apoptoses after androgen withdrawal. Importantly, the physiologic process of AWIA can be mimicked in NRP cells *in vitro*, by the addition of TGF β 1 to cultures previously differentiated in mitogen-poor media. NRP cells maintained in mitogen-rich media are resistant to TGF β 1 induced apoptosis (28). This is due at least in part to activation of the Akt/mTOR pathway, which suppresses Smad3 activation (29). Our previous observation that castration-

induced down-regulation of FLIP in the rat prostate immediately precedes the onset of apoptosis, suggested that FLIP might have a functional role in regulating the apoptosis of prostate epithelium that occurs following androgen withdrawal. The current report tests this possibility, employing TGF β 1 induced apoptosis of NRP cells as a model for AWIA in the rat prostate.

Results

NRP-152 cells grown in rich media (GM2), then re-plated in low growth factor media (GM3), rapidly differentiate to a luminal (secretory) epithelial phenotype, both morphologically and biochemically (27). The proliferation of these cells slows markedly from a doubling time of less than a day to more than three days (Figure 1a, cross-hatched bars and data not shown (DNS)) but they do not apoptose (Figure 1a, squares). If, after 3 h in differentiation media, the cells are treated with 5 ng TGF β 1/mL, the adherent live cells decline by about half at two days while the apoptotic cells increase ten-fold relative to the untreated controls (Figure 1A, black bars and circles). Nucleosomal cleavage of DNA isolated after TGF β 1 treatment shows that the apoptosis is evident as early as 10 h after TGF β 1 addition (Figure 1b). Within 6 h, the activity of caspase-3 in TGF β 1 treated cells is elevated relative to untreated NRP-152 cells. Caspase-3 activity continues to rise through 36 h TGF β 1 treatment (Figure 1c). Immunoblots of nuclear extracts of NRP cells either untreated or treated with TGF β 1 for up to 72 h (Figure 1d), show that one substrate of caspase-3, poly(ADP-ribose)polymerase (PARP), is also cleaved in the TGF β 1 treated cells with a maximum at 36 h treatment. The initial high level of PARP cleavage at 12 h is not likely due to TGF β 1 effects on cells, but to cells that fail to differentiate and die as a result of the low level of growth factors in the differentiation media. Since we have previously found that FLIP is reduced during rat prostate apoptosis, cytoplasmic protein isolated from a

combination of adherent and floating cells at each time-point was examined by immunoblotting for FLIP. FLIP protein is low when the NRP cells are re-plated in differentiation media and subsequently increases 24-60 h after differentiation (Figure 1e). Differentiating NRP cells treated with TGF β 1, in contrast, express low FLIP levels for up to 48 h following treatment.

The decline in FLIP levels in response to TGF β 1 may leave NRP cells more vulnerable to apoptosis. To test this hypothesis, we transfected a constitutively expressed FLIP gene into NRP cells and selected clonal lines expressing varying levels of FLIP. FLIP is expressed in two isoforms: FLIP long (FLIP_L) which has two DED domains at the amino-terminus, followed by a caspase domain containing inactivating mutations, and FLIP short (FLIP_S), which contains only the two DED domains. Both FLIP_L and FLIP_S can be detected by our DED-directed anti-FLIP antibody (DNS), but only the long form is found in extracts of NRP cells. High level over-expression of FLIP_L has been previously reported to induce apoptosis via a mechanism that is poorly understood (30-32). Therefore, we transfected NRP cells with either a HA-tagged FLIP_S construct, or the corresponding empty vector, and isolated clonal lines. To assess apoptotic response, cells were differentiated in GM3 and treated with TGF β 1. Differentiated parental NRP cultures treated with TGF β 1 contain more than three times as many apoptotic cells as untreated differentiated cultures (Figure 2a, bar labeled P). Cultures from clones transfected with vector alone display somewhat less apoptotic response to TGF β 1 induced cell death (Figure 2a, V1; Figure 4a, V2 and DNS). This may be due to extended passaging during the selection process, which can produce clones partially resistant to TGF β 1 (27). Of 48 G418-resistant clones screened for FLIP_S, one showed high and two others very low levels of anti-HA immunoreactivity (Figure 2b and DNS). When the resistant but non-expressing clones were assessed for TGF β 1 induced apoptosis, a range from 150-350% (relative to the untreated, differentiated control; see Materials and Methods) was seen (Figure 2a). Two clones expressing

low levels of FLIP (14 and 42) had a level of apoptosis equal to 250% of the untreated control, while the one clone (12) expressing a high level of FLIP_S showed no increase in TGFβ1 induced apoptosis (Figure 2a). Similarly, when DNA was isolated from these clones 72 h after TGFβ1 treatment, internucleosomal cleavage was evident in samples from parental (P), vector-transfected (V), low expressing (14, 42) and non-expressing (32, 37) clones, but there was no cleavage of the DNA isolated from the clone (12) expressing high levels of FLIP_S (Figure 2c).

Cytosolic extracts were prepared from differentiated clones and caspase-3 enzymatic activity was determined (Figure 3b). The induction of caspase activity in TGFβ1 treated versus untreated cells ranged from 5- to 15-fold in parental (P), vector only (V1), and low expressing clones (32, 37). The clone (12) expressing high levels of FLIP_S showed no induction of caspase-3 activity (Figure 3b). The level of induction of caspase-3 activity correlated closely with the level of TGFβ1 induced apoptosis (compare Figures 3a and 3b). The extracts used in Figure 3b were immunoblotted using an antibody that detects both full-length caspase-3 (32 kD) and its active fragment (17 kD). The top panel of Figure 3c shows that TGFβ1 treated and untreated extracts have approximately equal amounts of caspase-3, but a long exposure of the lower portion of the blot shows that the 17 kD fragment is induced in extracts from all of the TGFβ1 treated clones except clone 12 (Figure 3c, lower panel). Similarly, the caspase-3 substrate PARP is cleaved from 117 kD to an 84 kD fragment after TGFβ1 treatment in all clones except clone 12 (Figure 3d).

There is a strong correlation between FLIP_S transgene expression, caspase-3 activity and apoptosis for this set of clones, but the variability in TGFβ1 response after selection and the lack of response in the low expressing clones suggested that analysis of an additional set of FLIP_S expressing clones might be informative. We therefore isolated an additional set of clones. Two of 48 G418 resistant clones in this second set expressed relatively high levels of FLIP_S (Figure

4b, top panel) with clone 66 expressing several times more FLIP_S than clone 48. Extended exposure of the immunoblot reveals that three additional clones display low level expression (Figure 4b, second panel). Each of these low expressing clones has similar levels of endogenous FLIP_L when normalized to actin (Figure 4b, third and fourth panels). Additional anti-FLIP immunoblots (DNS) demonstrated that clones 48 and 66 expressed FLIP_S at levels approximately equivalent to the level of endogenous FLIP_L, while clones 61, 43, 53 produce significantly less of the short isoform relative to the level of the endogenous long isoform. Apoptosis in response to TGFβ1 ranged from 280-375% for the vector clones (Figure 4a, V2 and DNS) and non-expressing clones (44, 51 in Figure 4a and DNS). The three low expressing clones had an intermediate level of apoptosis (140-180%) while the clone with a higher level of FLIP_S expression (48) had 130%, and the highest expressor (66) only 80%, of the TGFβ1 induced apoptosis relative to untreated controls (Figure 4a). Again, caspase-3 activity was highly induced (~15-fold) after TGFβ1 treatment of the vector containing and FLIP_S non-expressing clones (Figure 4c). The low expressing clones displayed attenuated induction (~2-fold), while the two high expressors showed no induction of caspase-3 activity (Figure 4c). Induction of PARP cleavage was only seen in the vector containing and the non-expressing clones (V2, 44, 51 in Figure 4d) while there was no TGFβ1 induced cleavage in any of the FLIP_S expressing clones. Thus, Figures 2-4 indicate that forced over-expression of FLIP_S protects NRP cells from TGFβ1 induced caspase activation and cell death.

FLIP is thought to block DR induced activation of the apical caspases -8 and -10. Since the Fas DR has been implicated in prostate apoptosis (33-35), we sought to determine if TGFβ1 induced apoptosis requires Fas signaling, by employing Fas-Fc to block the FasL-Fas interaction. Initial experiments using human Fas-Fc did not block cell death (DNS). Since rat Fas differs from human Fas, a chimera (rFas-Fc) containing a CD5 leader, the extracellular domain of rat

Fas fused to Fc and a carboxyl-terminal HA tag was expressed in 293T cells and purified on a protein A column (Figure 5a). Jurkat cells were then used to validate the molecular reagents (Figure 5b). Specifically, treatment with 200 pg/ml of membrane bound FasL (mFasL) induced cell death after 18 h (diagonal striped bars). Further addition of Fc had no effect, while rFas-Fc completely blocked mFasL mediated killing. If TGF β 1 induced apoptosis is mediated via the FasL-Fas pathway, the kinetics of death should be similar for mFasL and TGF β 1. Indeed, when NRP cells are treated with mFasL, there is very little cell death apparent until 48 h and it is maximal at 72 h (Figure 5c and DNS). In addition, NRP cells are less sensitive than Jurkat cells to mFasL, with a ten-fold higher dose (2 ng/ml) required for complete NRP killing (DNS). The addition of rFas-Fc blocks mFasL induced killing (Figure 5c, compare black and horizontally striped bars), but does not effect killing at two doses of TGF β 1 (1 ng/ml, diagonally striped bars; 5 ng/ml, checkered bars). Similarly, neither 5- nor 25-fold increases in the amount of rFas-Fc significantly reduced the apoptosis induced by 1 ng/ml TGF β 1 in these cells (Figure 5d).

Since rFas-Fc was unable to block TGF β 1 induce apoptosis, we examined whether TRAIL, which acts via FLIP-inhibitable caspase 8 or caspase 10, might be induced by TGF β 1 and blocked by FLIP. Specifically, since TRAIL kills neoplastic and normal human prostate epithelial cells (18) via activation of the apical caspases (36), we examined its role in TGF β 1 mediated apoptosis. TRAIL can bind two death-inducing receptors, DR4 and DR5, as well as three decoy receptors and OPG (37) and Fc fusions of the extracellular domains of these receptors block TRAIL-induced cell death (18). As in Figure 5, we employed Jurkat cells to demonstrate the utility of DR4-Fc and DR5-Fc. Although treatment with DR4-Fc alone was partially toxic to Jurkat cells, DR4-Fc was able to block TRAIL induced death, particularly at lower concentrations of TRAIL (Figure 6a). DR5-Fc was also able to block TRAIL induced cell death (Figure 6b). TRAIL killed NRP cells but, as was the case for mFasL, only at significantly

higher concentrations relative to the dose that was effective in killing Jurkat cells (Figure 6c). Since DR4-Fc and DR5-Fc were most effective blocking lower TRAIL doses, we treated NRP cells with varying doses of TGF β 1, from 0.1 ng/ml, which is sub-lethal, up to 5 ng/ml and found the minimum concentration necessary to induce apoptosis is 0.5 ng/ml (Figure 6d-e, solid bars). As was the case for the Jurkat cells, DR4-Fc treatment of NRP cells was partially toxic in the absence of TGF β 1 (Figure 6d, bars at far left). However, neither DR4-Fc nor DR5-Fc inhibited TGF β 1 induced apoptosis of NRP cells (Figure 6d-e, solid vs. striped bars). Since the two TRAIL receptors might have complementary roles in signaling (38), we also employed DR4-Fc and DR5-Fc in combination, but again observed no effect on TGF β 1-induced cell death (Figure 6f).

Finally, we sought to determine if growth factors that modulate the growth and differentiation of NRP cells also regulate FLIP expression. Insulin and epidermal growth factor (EGF) both stimulate NRP proliferation in the presence of 10% fetal bovine serum (26), but only insulin (as well as the related growth factor IGF-1) inhibits the differentiation of NRP cells from the basal to the luminal phenotype (27). Insulin addition to the cell medium during differentiation effectively blocks TGF β 1 induced apoptosis as reported previously (28, 29), while EGF addition does not (Figure 7a, striped bars). Both insulin and EGF induce an increase in the level of FLIP_L but the kinetics are distinct. Specifically, when NRP cells are grown in GM3 differentiation media plus insulin, FLIP_L protein levels increase significantly after 6 h (Figure 7b, lanes 3-4) and remain elevated at 24 h and 48 h (Figure 7c, lanes 2 and 6). In contrast, when EGF is added to differentiating NRP cultures, FLIP_L levels rise only slightly after 6 h (Figure 7b, lanes 1-2) before increasing significantly at 24 h and 48 h (Figure 7d, lanes 2 and 6). Figure 1 demonstrated that treatment of differentiated NRP cells with TGF β 1 down-regulates FLIP_L protein levels and coordinately induces apoptosis. Similarly, Figure 7c-d (lanes 3-4 and 7-8)

shows that TGF β 1 reduces FLIP_L expression and induces PARP cleavage, a marker of apoptotic caspase activation. Insulin prevents the TGF β 1 induced reduction of FLIP_L at both 24 h (Figure 7c, lanes 1 and 3) and 48 h (Figure 7c, lanes 5 and 7) and effectively prevents PARP cleavage. EGF is not effective at reducing FLIP_L expression and is only partly effective at inhibiting PARP cleavage (Figure 7c, lanes 1,3, 5 and 7). Thus, treatment of NRP cells with these EGF and Insulin during differentiation modulates FLIP_L levels and further demonstrates that TGF β 1 induced apoptosis is inversely correlated with the level of FLIP_L expression.

Discussion

Androgen withdrawal induced cell death appears to be mediated, at least in part, by TGF β that is secreted in response to androgen ablation. Significantly, the NRP-152 cell line apoptoses when treated with TGF β 1, as demonstrated by caspase activation, DNA fragmentation and a decline in cell number (Figure 1). Since we previously demonstrated that both FLIP mRNA (2) and protein levels (KLN and JJK, unpublished observations) decline following castration in rats, we sought to determine whether enforced, continuous expression of FLIP would be sufficient to block TGF β 1 induced apoptosis of NRP cells. We chose to express FLIP_S since FLIP_L over-expression has been reported to spontaneously induces cell death in some cell lines. While we do not necessarily believe that FLIP_S is the relevant FLIP isoform in NRP cells (indeed we have not detected FLIP_S in NRP cells; see Figure 1) we were concerned that our expression vector might be more potent than the endogenous promoter, running the risk of over-expression. When NRP cells were stably transfected with an HA-tagged, constitutively expressed FLIP_S gene, evidence of TGF β 1 induced apoptosis was absent (Figures 2-4). Further, NRP clones expressing very low levels of FLIP_S showed no evidence of apoptosis, while clonal cell lines expressing moderate

levels of FLIP_S showed an intermediate phenotype, suggesting the dose of FLIP_S expression is crucial in determining its effectiveness in blocking cell death in normal prostate cells. This stoichiometry dependent effect of FLIP_S is consistent with the idea that this protein acts in a dominant inhibitory manner to block the function of caspase-8.

If FLIP_S antagonizes TGFβ1 induced apoptosis by inhibiting caspase-8, both proximal and distal caspase mediated cleavage events should be attenuated. As expected, TGFβ1 treatment of untransfected NRP cells induced significant cleavage of both caspase-3 and PARP, a caspase-3 substrate and apoptosis marker, as well as the caspase-3 peptide substrate (Figure 1). However, when we examined caspase activation in TGFβ1 treated FLIP_S expressing clones, we found little or no increase in caspase-3 activity (Figures 3-4). Furthermore, neither caspase-3 itself nor PARP are cleaved in the clones expressing intermediate or high levels of exogenous FLIP_S (Figures 3-4 and DNS). Taken together, these data indicate that FLIP_S expressing clones which are refractory to TGFβ1 induced cell death are not undergoing key biochemical changes that normally accompany apoptosis in NRP cells.

Proximally, we sought to measure caspase-8 activation, since caspase-8 is the likely target of the anti-apoptotic action of FLIP_S. In other TGFβ1 sensitive human cells, immunoblotting of treated cells with an antibody directed against human caspase-8 detected a slight increase in the caspase-8 cleavage while enzymatic assays revealed a small increase in caspase-8 activity (39). Unfortunately, neither this human antibody nor other antibodies tested detect rat caspase-8 active fragments (DNS) and we have not been able to identify a suitably sensitive antibody directed against rat caspase-8. Thus, we also assayed for cleavage of caspase peptide substrates. While we could readily detect an increase in caspase-8 activity at late (36-48 h) time-points, we could not detect activation of either caspase-8 (or -9) at 6, 12 or 18 h following TGFβ1 addition (DNS). Moreover, the caspase-8 and -9 activities observed at late

time-points were eliminated when we included an inhibitor of caspase-3, which is highly induced in these lysates (Figure 1c) and is known to cross-cleave both the IETD (caspase-8) and LEHD (caspase-9) substrates (DNS). The relatively low levels of TGF β 1 induced caspase-8 activity, which may be a result of the comparatively slow onset of cell death in these prostate epithelial cells versus T-cells, prevented us from determining if FLIP_S over-expression can indeed inhibit caspase-8 activity.

Since NRP apoptosis is blocked by FLIP_S, and FLIP_S is thought to inhibit apical caspases bound to death receptors, TGF β 1 may act by inducing (or stabilizing) the expression of a death receptor ligand. This can be tested by exploiting the observation that fusions between the extracellular domain of a receptor and the immunoglobulin Fc domain block DR ligand induced apoptosis. To determine if FasL is involved in TGF β 1 induced NRP apoptosis, we measured cell death in the presence of rFas-Fc, which blocks the interaction between FasL and Fas. While FasL induced apoptosis in NRP cells, rFas-Fc protein failed to block TGF β 1 induced NRP cell death (Figure 5). TRAIL is thought to be a potent inducer of prostate cell death (20) and TRAIL receptors are expressed in normal prostate epithelial cells (18, 40) as well as a variety of prostate cancer cell lines (41, 42). Blocking DR5 rescues TRAIL-induced apoptosis in normal human prostate epithelial cells (18). Although TRAIL induced NRP apoptosis, blocking experiments with two TRAIL receptor-Fc fusion proteins individually or in combination failed to inhibit TGF β 1 induced cell death (Figure 6). While our data argue against a role for TRAIL in TGF β 1 mediated NRP apoptosis, it remains possible that the human TRAIL receptor-Fc fusions we employed failed to block rat TRAIL signaling because of sequence differences between the human and rat TRAIL receptors. Consistent with this possibility, others have reported that human DR4-Fc inhibits TGF β 1 induced apoptosis of human hepatoma cell lines (43). However, there is also precedence for the possibility that FLIP blocks TGF β 1 induced apoptosis in a

receptor-independent manner. Specifically, TGF β 1 treatment of SNU-620 gastric carcinoma cells activates caspase-8 and induces caspase-8 dependent apoptosis, but this effect is not blocked by Fas-Fc nor is it enhanced by FasL (44). Because TGF β 1 induced cell death in SNU-620 cells requires functional FADD, FLIP would be expected to act in a dominant inhibitory manner in this cell line. Thus, a similar mechanism could be operative in NRP cells.

Although the remaining DR ligands (TNF and TWEAK) are also potential candidates to mediate TGF β 1 regulated cell death, we believe this is unlikely. TWEAK is a relatively inefficient inducer of apoptosis (45) and there are no reports of its activity in prostate epithelial cells. TNF can induce cell death as well as cell survival, dependent in part on the nature of the receptor complexes formed in response to ligand binding (46). While the mechanism controlling the decision to apoptose or survive is unclear, NF κ B activation is an important determinant. In most prostate epithelial cells, including normal epithelial cells and the PC-3 and DU145 cell lines, NF κ B is activated and TNF does not induce significant apoptosis (47, 48). The LNCaP cell line undergoes apoptosis in response to TNF, but is defective in the regulation of NF κ B and therefore may be a poor model for normal prostate epithelium (47). Thus, it seems unlikely that TNF mediates cell death in normal prostate epithelial cells.

Finally, to better understand how the process of NRP differentiation sensitizes cells to TGF β 1 induced apoptosis, we investigated the modulation of FLIP expression by mitogens. Insulin and IGF-1 protect against TGF β 1 induced apoptosis, while EGF does not (Figure 7 and (29)). IGF-1 and insulin, which signal via similar pathways, act in two ways: inhibiting the activation of Smad3, and maintaining the intracellular level of FLIP, even in the presence of TGF β 1 (Figure 7). Both insulin and IGF-1 induce Akt phosphorylation, inhibiting the activity of Smad3 (49) and Bad (50), and up-regulating FLIP (Figure 7). Phospho-Akt, but not EGF stimulated phospho-ERK, is associated with an increased proliferative index in prostate tumors

(51). This suggests that the resistance of insulin stimulated NRP cells to apoptosis, perhaps acting via sustained expression of FLIP, is reflective of changes in human tumors.

Materials and Methods

Reagents and Antibodies

Caspase substrates (Biomol, Plymouth Meeting, PA), mFasL (UBI, Charlottesville, VA), 'super killer' mouse TRAIL, DR4-Fc and DR5-Fc (Alexis Biochemicals, San Diego, CA), TGF β 1 (R&D systems, Minneapolis, MN), anti-actin (AC-10, Sigma, St. Louis, MO), anti-PARP (C2.10, Enzyme Systems, Livermore, CA) were purchased from the indicated suppliers. Antibody against the rat FLIP_L amino-terminal peptide QVEESLDEDEKEC was prepared by immunizing rabbits and then purified by peptide affinity chromatography.

Cell culture, transfection and apoptosis assay

Passage 27 NRP-152 cells were maintained as described (26). Briefly, the cells were cultured in GM2 (Dulbecco's modified Eagle's medium/F12 medium containing 5% fetal bovine serum, 20 ng/ml epidermal growth factor (BD Biosciences, San Jose, CA), 0.1 mM dexamethasone (Sigma), 10 ng/ml cholera toxin (Sigma), and 350 nM insulin (Biosource, Camarillo, CA)) and passaged before reaching confluence. NRP cells were discarded after 15 passages, except the FLIP expressing clones, which range from 20 to 25 passages after selection. Apoptosis assays were performed in differentiation media (GM3; Dulbecco's modified Eagle's medium/F12 containing 1% calf serum, 15 mM HEPES, and 0.1 mM dexamethasone) using 5 ng/ml TGF β 1 or vehicle (4 mM HCl, 1 mg/ml bovine serum albumin).

The rat FLIP_S cDNA was cloned by RT-PCR into pBluescript, transferred to a vector containing a carboxyl-terminal HA tag and then into the KpnI and ApaI sites of pcDNA3.1 (Invitrogen, Carlsbad, CA) to create p-ratFLIP_SHA. This plasmid was transfected with

Lipofectamine Plus (Life Technologies, Inc., Gaithersburg, MD) and transfectants selected using G418 (GibcoBRL, Grand Island, NY) at 200 ng/ml in GM2.

After TGF β 1 treatment, NRP cells that adhere to tissue culture plates after two PBS washes exclude trypan blue, possess nuclei that appear non-apoptotic by DAPI staining, and show no caspase activation by immunoblotting analysis. In contrast, the detached cells are uniformly apoptotic when recovered from the GM3 media and PBS washes. These detachable (floating) cells are apoptotic by DNA laddering, caspase activation by immunoblot analysis, and DAPI nuclear staining (52). Quantification of NRP detachable cells and adherent cells released by trypsin treatment after the PBS washes using a Coulter counter was therefore used as a measure of TGF β 1 induced apoptosis of NRP cells. The percent apoptotic cells (% apoptosis) represents the ratio of detachable cells in the TGF β 1 treated dishes relative to the untreated control dishes. TGF β 1 treatment of differentiated NRP cells induces a three- to four-fold increase in the number of floating cells and, hence, 300-400% apoptosis (for example bars labeled P in Figures 2a and 3a)

DNA isolation and labeling

Attached and floating NRP cells were pooled and DNA was extracted by lysing cells in 7M guanidine hydrochloride followed by further purification using the Wizard system (Promega) as described previously (2). DNA fragments were end-labeled with ^{32}P -ddATP and terminal deoxynucleotide transferase (TdT) as described (53). The labeled DNA was fractionated on a 2% agarose gel and the gel was dried and autoradiographed.

Caspase activity assays

NRP cells were treated with TGF β 1 or vehicle for 36 h. Adherent and floating cells were pooled, harvested, washed with PBS and counted. The cells were lysed in 20 mM EDTA, 5 mM Tris, pH 8.0, and 0.5% Triton X-100 to isolate caspase-containing cytoplasm. Extract from

400,000 cells was diluted into 0.1% CHAPS, 50 mM DTT, 50 mM HEPES, pH 7.4, 100 mM NaCl, 1 mM EDTA and 10% glycerol, 50 μ M DEVD-pNA (caspase-3 substrate), 100 nM IETD-CHO (caspase-8 inhibitor), 5 nM YVAD-CHO (caspase-1 inhibitor) and incubated at 37°C. Production of pNA was monitored at 405 nm for 3 h and activity was determined from the slope of the curve in the linear range for each sample. Each sample was assayed in triplicate.

Purification of rat Fas-Fc

Full-length rat Fas was cloned by RT-PCR into pBluescript and the ECD excised and cloned into pB-CD5Lneg1 (54) containing the CD5 leader sequence and the human Fc domain. This construct and the CD5L-Fc only fragment were excised and separately inserted into pMT2T-HA to create pMT2T-ratFasECD-Fc-HA and the corresponding Fc-HA construct. HEK293T cells were transfected with either the rFas-Fc or the Fc only construct and the protein was purified from the media via Protein A (BioRad, Hercules, CA) chromatography.

Cell growth assay

In some cases cell growth was assessed by WST-1 (Boehringer, Mannheim, Germany) conversion to formazan. NRP or Jurkat cells were plated in 96-well plates at 2,000 cells/well in GM3 or 10,000 cells/well in RPMI/10% FBS, respectively. Receptor-Fc protein was added at the indicated concentration at the time of plating. After 3 h, FasL, TRAIL, TGF β 1 or vehicle were added, as indicated. After an additional 18 h (Jurkat) or 72 h (NRP), WST-1 was added, plates were incubated at 37°C and absorbance at 450 nm (less background absorbance at 600 nM) was measured in a microplate reader. Conversion rates were derived from the slope of the curve in the linear range for each sample.

Acknowledgements

This research was supported by grant PC030937 from the US Army Prostate Cancer Research Program.

References

1. Isaacs JT. Antagonistic effect of androgen on prostatic cell death. *Prostate* 1984;5:545-57.
2. Nastiuk KL, Kim JW, Mann M, Krolewski JJ. Androgen regulation of FLICE-like inhibitory protein gene expression in the rat prostate. *J Cell Physiol* 2003;196:386-93.
3. Colombel MC, Buttyan R. Hormonal control of apoptosis: the rat prostate gland as a model system. *Methods Cell Biol* 1995;46:369-85.
4. Brodin G, ten Dijke P, Funa K, Heldin CH, Landstrom M. Increased smad expression and activation are associated with apoptosis in normal and malignant prostate after castration. *Cancer Res* 1999;59:2731-8.
5. Kyprianou N, Isaacs JT. Expression of transforming growth factor-beta in the rat ventral prostate during castration-induced programmed cell death. *Mol Endocrinol* 1989;3:1515-22.
6. Kim IY, Ahn HJ, Zelner DJ, Park L, Sensibar JA, Lee C. Expression and localization of transforming growth factor-beta receptors type I and type II in the rat ventral prostate during regression. *Mol Endocrinol* 1996;10:107-15.
7. Kundu SD, Kim IY, Yang T, Doglio L, Lang S, Zhang X, et al. Absence of proximal duct apoptosis in the ventral prostate of transgenic mice carrying the C3(1)-TGF-beta type II dominant negative receptor. *Prostate* 2000;43:118-24.

8. Tang B, de Castro K, Barnes HE, Parks WT, Stewart L, Bottinger EP, et al. Loss of responsiveness to transforming growth factor beta induces malignant transformation of nontumorigenic rat prostate epithelial cells. *Cancer Res* 1999;59:4834-42.
9. Martikainen P, Kyprianou N, Isaacs JT. Effect of transforming growth factor-beta 1 on proliferation and death of rat prostatic cells. *Endocrinology* 1990;127:2963-8.
10. Coyle B, Freathy C, Gant TW, Roberts RA, Cain K. Characterization of the transforming growth factor-beta 1-induced apoptotic transcriptome in FaO hepatoma cells. *J Biol Chem* 2003;278:5920-8.
11. Nagata S. Apoptosis by death factor. *Cell* 1997;88:355-65.
12. Nagata S, Golstein P. The FAS death factor. *Science* 1995;267:1449-56.
13. Peter ME, Krammer PH. The CD95(APO-1/Fas) DISC and beyond. *Cell Death Differ* 2003;10:26-35.
14. Xerri L, Devilard E, Hassoun J, Mawas C, Birg F. Fas ligand is not only expressed in immune privileged human organs but is also coexpressed with Fas in various epithelial tissues. *Mol Path* 1997;50:87-91.
15. Sasaki Y, Ahmed H, Takeuchi T, Moriyama N, Kawabe K. Immunohistochemical study of Fas, Fas ligand and interleukin-1 β converting enzyme expression in human prostatic cancer. *Br J Urol* 1998;81:852-5.
16. Bin L, Li X, Xu LG, Shu HB. The short splice form of Casper/c-FLIP is a major cellular inhibitor of TRAIL-induced apoptosis. *FEBS Lett* 2002;510:37-40.
17. MacFarlane M. TRAIL-induced signalling and apoptosis. *Toxicol Lett* 2003;139:89-97.
18. Nesterov A, Ivashchenko Y, Kraft AS. Tumor necrosis factor-related apoptosis-inducing ligand (TRAIL) triggers apoptosis in normal prostate epithelial cells. *Oncogene* 2002;21:1135-40.

19. Yu R, Mandlekar S, Ruben S, Ni J, Kong AN. Tumor necrosis factor-related apoptosis-inducing ligand-mediated apoptosis in androgen-independent prostate cancer cells. *Cancer Res* 2000;60:2384-9.
20. Voelkel-Johnson C, King DL, Norris JS. Resistance of prostate cancer cells to soluble TNF-related apoptosis-inducing ligand (TRAIL/Apo2L) can be overcome by doxorubicin or adenoviral delivery of full-length TRAIL. *Cancer Gene Therap* 2002;9:164-72.
21. Kelly MM, Hoel BD, Voelkel-Johnson C. Doxorubicin pretreatment sensitizes prostate cancer cell lines to TRAIL induced apoptosis which correlates with the loss of c-FLIP expression. *Cancer Biol Ther* 2002;1:520-7.
22. Siegmund D, Hadwiger P, Pfizenmaier K, Vornlocher HP, Wajant H. Selective inhibition of FLICE-like inhibitory protein expression with small interfering RNA oligonucleotides is sufficient to sensitize tumor cells for TRAIL-induced apoptosis. *Mol Med* 2002;8:725-32.
23. Zhang X, Jin TG, Yang H, DeWolf WC, Khosravi-Far R, Olumi AF. Persistent c-FLIP(L) expression is necessary and sufficient to maintain resistance to tumor necrosis factor-related apoptosis-inducing ligand-mediated apoptosis in prostate cancer. *Cancer Res* 2004;64:7086-91.
24. Rippo MR, Moretti S, Vescovi S, Tomasetti M, Orecchia S, Amici G, et al. FLIP overexpression inhibits death receptor-induced apoptosis in malignant mesothelial cells. *Oncogene* 2004;23:7753-60.
25. Abedini MR, Qiu Q, Yan X, Tsang BK. Possible role of FLICE-like inhibitory protein (FLIP) in chemoresistant ovarian cancer cells in vitro. *Oncogene* 2004;23:6997-7004.
26. Danielpour D, Kadomatsu K, Anzano MA, Smith JM, Sporn MB. Development and characterization of nontumorigenic and tumorigenic epithelial cell lines from rat dorsal-lateral prostate. *Cancer Res* 1994;54:3413-21.

27. Danielpour D. Transdifferentiation of NRP-152 rat prostatic basal epithelial cells toward a luminal phenotype: regulation by glucocorticoid, insulin-like growth factor-I and transforming growth factor-beta. *J Cell Sci* 1999;112:169-79.
28. Hsing AY, Kadomatsu K, Bonham MJ, Danielpour D. Regulation of apoptosis induced by transforming growth factor-beta1 in nontumorigenic rat prostatic epithelial cell lines. *Cancer Res* 1996;56:5146-9.
29. Song K, Cornelius SC, Reiss M, Danielpour D. Insulin-like growth factor-I inhibits transcriptional responses of transforming growth factor-beta by phosphatidylinositol 3-kinase/Akt-dependent suppression of the activation of Smad3 but not Smad2. *J Biol Chem* 2003;278:38342-51.
30. Goltsev YV, Kovalenko AV, Arnold E, Varfolomeev EE, Brodianskii VM, Wallach D. CASH, a novel caspase homologue with death effector domains. *J Biol Chem* 1997;272:19641-4.
31. Inohara N, Koseki T, Hu Y, Chen S, Nunez G. CLARP, a death effector domain-containing protein interacts with caspase-8 and regulates apoptosis. *Proc Natl Acad Sci USA* 1997;94:10717-22.
32. Shu HB, Halpin DR, Goeddel DV. Casper is a FADD- and caspase-related inducer of apoptosis. *Immunity* 1997;6:751-63.
33. Hedlund TE, Duke RC, Schleicher MS, Miller GJ. Fas-mediated apoptosis in seven human prostate cancer cell lines: correlation with tumor stage. *Prostate* 1998;36:92-101.
34. Hedlund TE, Meech SJ, Srikanth S, Kraft AS, Miller GJ, Schaack JB, et al. Adenovirus-mediated expression of Fas ligand induces apoptosis of human prostate cancer cells. *Cell Death Diff* 1999;6:175-82.

35. Rokhlin OW, Bishop GA, Hostager BS, Waldschmidt TJ, Sidorenko SP, Pavloff N, et al. Fas-mediated apoptosis in human prostatic carcinoma cell lines. *Cancer Res* 1997;57:1758-68.
36. Rokhlin OW, Guseva NV, Tagiyev AF, Glover RA, Cohen MB. Caspase-8 activation is necessary but not sufficient for tumor necrosis factor-related apoptosis-inducing ligand (TRAIL)-mediated apoptosis in the prostatic carcinoma cell line LNCaP. *Prostate* 2002;52:1-11.
37. Truneh A, Sharma S, Silverman C, Khandekar S, Reddy MP, Deen KC, et al. Temperature-sensitive differential affinity of TRAIL for its receptors. DR5 is the highest affinity receptor. *J Biol Chem* 2000;275:23319-25.
38. Leverkus M, Sprick MR, Wachter T, Denk A, Brocker EB, Walczak H, et al. TRAIL-induced apoptosis and gene induction in HaCaT keratinocytes: differential contribution of TRAIL receptors 1 and 2. *J Invest Dermatol* 2003;121:149-55.
39. Wallace CS, Withers GS, Weiler IJ, George JM, Clayton DF, Greenough WT. Correspondence between sites of NGFI-A induction and sites of morphological plasticity following exposure to environmental complexity. *Brain Res Mol Brain Res* 1995;32:211-20.
40. Vindrieux D, Devonec M, Benahmed M, Grataroli R. Identification of tumor necrosis factor-alpha-related apoptosis-inducing ligand (TRAIL) and its receptors in adult rat ventral prostate. *Mol Cell Endocrinol* 2002;198:115-21.
41. Munshi A, Pappas G, Honda T, McDonnell TJ, Younes A, Li Y, et al. TRAIL (APO-2L) induces apoptosis in human prostate cancer cells that is inhibitable by Bcl-2. *Oncogene* 2001;20:3757-65.
42. Sridhar S, Ali AA, Liang Y, El Etreby MF, Lewis RW, Kumar MV. Differential expression of members of the tumor necrosis factor alpha-related apoptosis-inducing ligand pathway in prostate cancer cells. *Cancer Res* 2001;61:7179-83.

43. Herzer K, Ganten TM, Schulze-Bergkamen H, Grosse-Wilde A, Koschny R, Krammer PH, et al. Transforming growth factor beta can mediate apoptosis via the expression of TRAIL in human hepatoma cells. *Hepatology* 2005;42:183-92.
44. Kim SG, Jong HS, Kim TY, Lee JW, Kim NK, Hong SH, et al. Transforming growth factor-beta 1 induces apoptosis through Fas ligand-independent activation of the Fas death pathway in human gastric SNU-620 carcinoma cells. *Mol Biol Cell* 2004;15:420-34.
45. Wiley SR, Winkles JA. TWEAK, a member of the TNF superfamily, is a multifunctional cytokine that binds the TweakR/Fn14 receptor. *Cytokine Growth Factor Rev* 2003;14:241-9.
46. Micheau O, Tschopp J. Induction of TNF receptor I-mediated apoptosis via two sequential signaling complexes. *Cell* 2003;114:181-90.
47. Chopra DP, Menard RE, Januszewski J, Mattingly RR. TNF-alpha-mediated apoptosis in normal human prostate epithelial cells and tumor cell lines. *Cancer Lett* 2004;203:145-54.
48. Mukhopadhyay A, Bueso-Ramos C, Chatterjee D, Pantazis P, Aggarwal BB. Curcumin downregulates cell survival mechanisms in human prostate cancer cell lines. *Oncogene* 2001;20:7597-609.
49. Remy I, Montmarquette A, Michnick SW. PKB/Akt modulates TGF-beta signalling through a direct interaction with Smad3. *Nat Cell Biol* 2004;6:358-65.
50. Wanke I, Schwarz M, Buchmann A. Insulin and dexamethasone inhibit TGF-beta-induced apoptosis of hepatoma cells upstream of the caspase activation cascade. *Toxicol* 2004;204:141-54.
51. Ghosh PM, Malik SN, Bedolla RG, Wang Y, Mikhailova M, Prihoda TJ, et al. Signal transduction pathways in androgen-dependent and -independent prostate cancer cell proliferation. *Endocr Related Cancer* 2005;12:119-34.

52. Chipuk JE, Bhat M, Hsing AY, Ma J, Danielpour D. Bcl-xL blocks transforming growth factor-beta 1-induced apoptosis by inhibiting cytochrome c release and not by directly antagonizing Apaf-1-dependent caspase activation in prostate epithelial cells. *J Biol Chem* 2001;276:26614-21.
53. Tilly JL, Hsueh AJW. Microscale autoradiographic method for the qualitative and quantitative analysis of apoptotic DNA fragmentation. *J Cell Physiol* 1993;154:519-26.
54. Zettlmeissl G, Gregersen JP, Duport JM, Mehdi S, Reiner G, Seed B. Expression and characterization of human CD4:immunoglobulin fusion proteins. *DNA Cell Biol* 1990;9:347-53.

Figure Legends

Figure 1 FLIP_L levels are reduced during TGFβ1 induced apoptosis of NRP cells. **(a)** Growth of differentiated NRP cells left untreated (solid bars and square symbol line) or treated with 5 ng/ml TGFβ1 (striped bars and circle symbol line). Bars indicate adherent cells (left axis) and lines indicate detached (floating) cells (right axis), each normalized as a percentage of the respective untreated control at 0 h. Error bars correspond to the standard error of the mean. **(b)** Fragmentation of chromosomal DNA in TGFβ1 treated NRP cells. Autoradiogram of an agarose gel containing TdT end-labeled nuclear DNA derived from NRP cells grown in growth medium (GM2), 3 h after re-plating in differentiation medium (DF), or after further incubation in differentiation medium containing 5 ng/ml TGFβ1 for the indicated time (h). **(c)** Caspase-3 activity in TGFβ1 treated NRP-152 cells. DEVD-pNA cleavage was measured in cytosolic extracts of differentiated NRP cells treated with 5 ng/ml TGFβ1 for the indicated time (h) as described in the Materials and Methods. Values were normalized to untreated, differentiated cells (n=4). Error bars correspond to the standard error of the mean. **(d)** Immunoblot of PARP cleavage. Nuclear extracts from differentiated NRP cells treated with 5 ng/ml TGFβ1 for the indicated time (h) (+), or left untreated (-), were probed with an anti-PARP antibody. The positions of the intact (PARP) and the amino-terminal cleavage product (cleaved) are indicated. **(e)** Immunoblot of FLIP_L protein levels. Cytoplasmic extracts from differentiated NRP cells treated with TGFβ1 as in **(d)** were immunoblotted with an anti-FLIP antibody. The positions of the full sized protein (FLIP_L) and the 43 kD amino-terminal cleavage product (cleaved) are indicated. The lane labeled “Control” corresponds to lysate from HEK293T cells transfected with a plasmid encoding FLIP_L.

Figure 2 Characterization of stable FLIP_S transfectants (set 1). **(a)** TGFβ1 induced apoptosis of FLIP_S transfectants. Cultures were shifted to differentiation media, treated with 5 ng/ml TGFβ1 and apoptotic (floating) cells counted after 72 h (n=4). Error bars correspond to the standard error of the mean. Bars correspond to the average apoptosis of parental NRP cell line (P), a clone transfected with the vector control (V1), and stable FLIP_S transfected clones (numbered) with varying levels of expression (see **(b)**). **(b)** FLIP_S and control transfectants described in **(a)** were grown in GM2 and protein extracts were immunoblotted with the anti-HA (upper panel), anti-FLIP (middle panel) or anti-actin (lower panel) antibodies. **(c)** Fragmentation of chromosomal DNA following TGFβ1 treatment of differentiated NRP transfectants. Similar to Figure 1b; clones were treated with 5 ng/ml TGFβ1 for 48 h. Lanes labeled as in **(a)** and **(b)**.

Figure 3 Caspase-3 activity of NRP transfectants (set 1). Cultures were differentiated, treated with 5 ng/ml TGFβ1 and portions harvested at either 36 h to assay for caspase activity **(b-d)** or at 72 h to quantitate apoptosis **(a)**. **(a)** Apoptosis of FLIP_S transfectants and controls (methods and labeling similar to Figure 2a). **(b)** Caspase-3 enzymatic activity of FLIP_S transfectants and controls was determined and plotted as in Figure 1c (n=3). Samples labeled as in **(a)**. **(c)** Caspase-3 cleavage in FLIP_S transfectants and controls. Cytoplasmic extracts from differentiated cultures (labeled as in **(a)**) treated with 5 ng/ml TGFβ1 for 36 h (+), or left untreated (-), were immunoblotted with an anti-caspase-3 antibody. The positions of the intact (Casp3) and the amino-terminal cleavage product (p17) are indicated. **(d)** PARP cleavage in FLIP_S transfectants and controls. Nuclear extracts of differentiated cultures treated as in **(c)** were immunoblotted with an anti-PARP antibody. The position of the 117 kD intact PARP and the 84 kD cleavage product (cleaved) are indicated.

Figure 4 Characterization of FLIP_S transfectants (set 2). **(a-b)** TGFβ1 induced apoptosis of FLIP_S transfectants. Additional stable FLIP_S transfected NRP cultures were analyzed as in Figure 2a-b. Minor low mobility bands in the third panel of (b) correspond to the 43 kD cleaved form of FLIP_L, as seen in the control lane of Figure 1e. **(c)** Caspase-3 enzymatic activity of FLIP_S transfectants and controls was determined and plotted as in Figure 3b (n=3). **(d)** PARP cleavage in FLIP_S transfectants and controls was determined as in Figure 3d.

Figure 5 Rat Fas-Fc blocks FasL, but not TGFβ1, induced cell death. **(a)** Anti-HA immunoblot of 1 μl purified HA tagged Fc (lane 1) and 1 μl Ha tagged rat Fas-Fc (lane 2) proteins. **(b)** Jurkat cell killing by mFasL is blocked by rFas-Fc. Jurkat cells were treated with diluent (solid bars), 200 pg/ml (diagonal striped bars), or 80 pg/ml (checkered bars) mFasL in the presence of diluent or the indicated amounts of Fc or rFas-Fc. After 18 h, WST-1 conversion to formazan was measured as described in Materials and Methods and normalized to untreated control Jurkat cells (n=4). Error bars correspond to the standard error of the mean. **(c)** NRP killing by mFasL is blocked by rFas-Fc, but killing by TGFβ1 is not. NRP cells were differentiated and then treated with diluent (solid bars), 1 ng/ml (diagonal striped bars) or 5 ng/ml (checkered bars) TGFβ1, or 2 ng/ml mFasL (horizontal striped bars) in the presence of diluent or the indicated amounts of Fc or Fas-Fc. After 72 h, WST-1 conversion to formazan was measured and plotted as in (b) (n=4). **(d)** NRP cell killing by TGFβ1 is not blocked by high doses of rFas-Fc. NRP cells were differentiated and then either treated with 1 ng/ml TGFβ1 or left untreated, in the presence of diluent (none) or the indicated amounts of Fc or Fas-Fc. After 72 h apoptotic (floating) cells were counted and the data plotted as in Figure 1a (n=3).

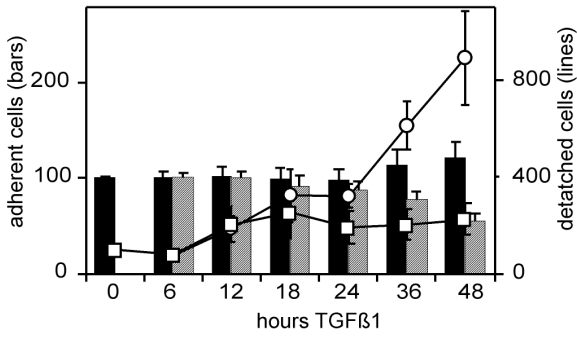
Figure 6 TRAIL R-Fc blocks TRAIL, not TGF β , induced cell death. **(a)** Jurkat cell killing by TRAIL is blocked by DR4-Fc. Jurkat cells were pre-treated with diluent (solid bars), or 250 ng/ml DR4-Fc (diagonal striped bars) for 3 h, followed by human TRAIL at the indicated concentrations. After 18 h, WST-1 conversion was measured and plotted as in Figure 5b (n=4). **(b)** Jurkat cell killing by TRAIL is blocked by DR5-Fc. Similar to **(a)**, except DR5-Fc was used. **(c)** NRP cells are killed by mTRAIL. NRP cells were treated with the indicated concentration of mouse TRAIL. After 72 h, WST-1 conversion was measured as in Figure 5b (n=4). **(d)** NRP cell killing by TGF β 1 is not blocked by DR4-Fc. NRP cells were pre-treated for 3 h with diluent (solid bars), or 250 ng/ml DR4-Fc (diagonal striped bars) and then treated with the indicated concentration of TGF β 1. After 72 h, WST-1 conversion was measured as in Figure 5b (n=4). **(e)** NRP cell killing by TGF β 1 is not blocked by DR5-Fc. Similar to **(d)**, except DR5-Fc was used. **(f)** NRP cell killing by TGF β 1 is not blocked by the combination of DR4-Fc and DR5-Fc. Similar to **(d)**, except that a combination of DR4-Fc and DR5-Fc (each at 250 ng/ml) was used.

Figure 7 Insulin increases FLIP_L levels in differentiating NRP-152 cells and blocks apoptosis. **(a)** Insulin blocks TGF β 1 induced apoptosis. NRP cells were differentiated for 6 h in the presence of diluent (none), EGF or insulin (at the concentrations used in GM2) and then treated with 5 ng/ml TGF β 1 (striped bars) or diluent (solid bars). After 72 h apoptotic (floating) cells were counted and the data plotted as in Figure 2a (n=3). **(b)** EGF and insulin differentially induce FLIP_L expression. NRP cells were differentiated for 6 h in either the absence or presence of insulin or EGF and appropriate extracts were immunoblotted for FLIP_L, PARP and actin. Representative sample of 3 separate experiments. **(c-d)** Effects of EGF and insulin on FLIP_L expression and PARP cleavage. NRP cells were differentiated for 6 h in either the absence or

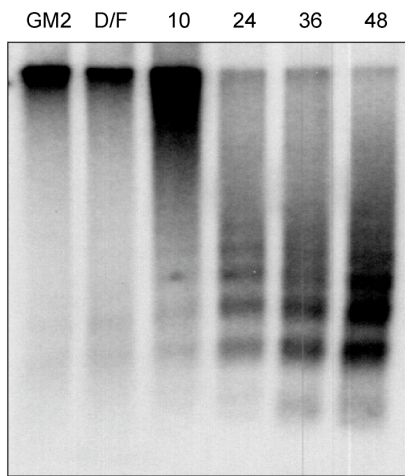
presence of insulin or EGF and then either left untreated or treated with 5 ng/ml TGF β 1 for 24 or 48 h, all as indicated. Appropriate extracts were immunoblotted as in **(b)**. Representative samples of three separate experiments.

Nastiuk, et al. Figure 1

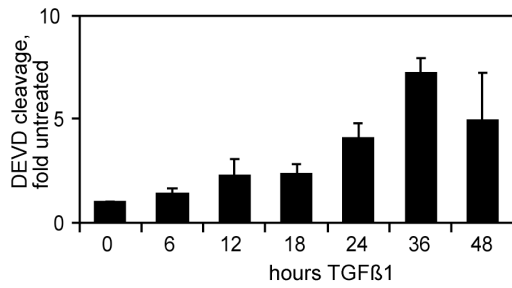
A



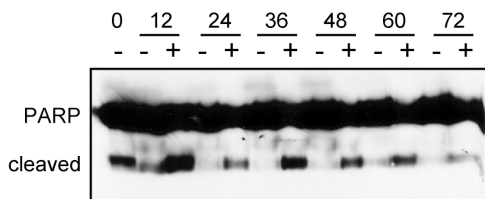
B



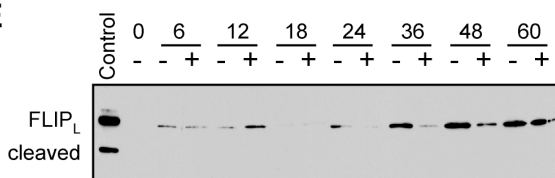
C



D

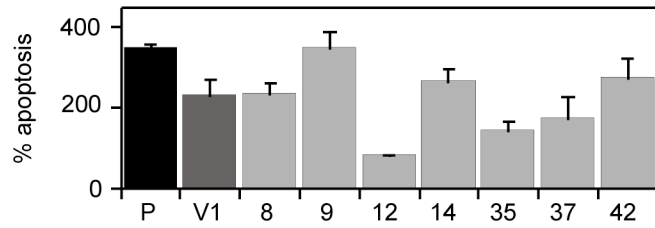


E

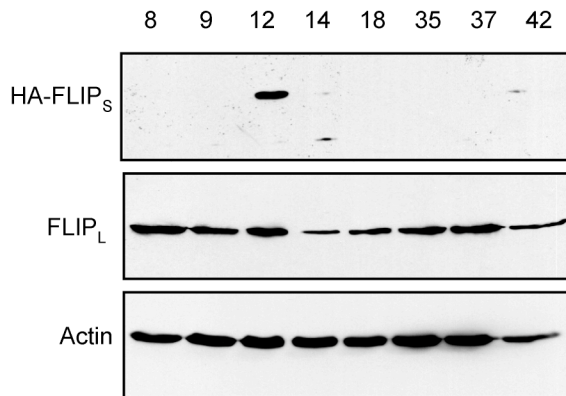


Nastiuk, et al. Figure 2

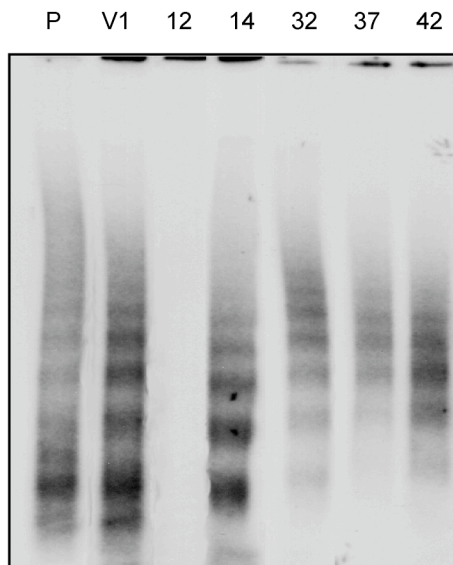
A



B

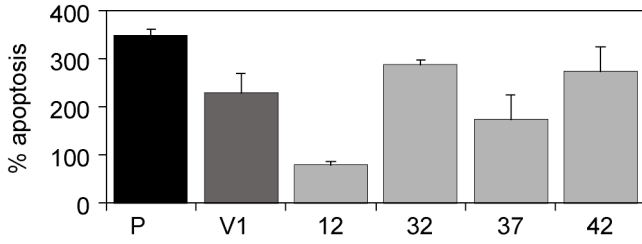


C

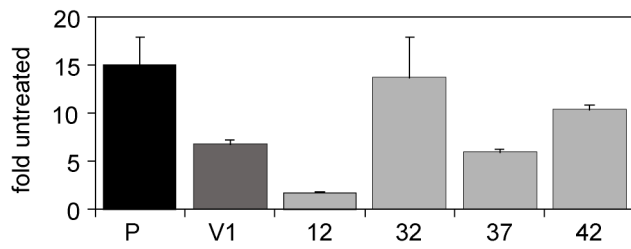


Nastiuk et al., Figure 3

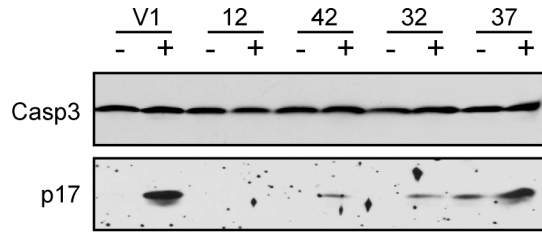
A



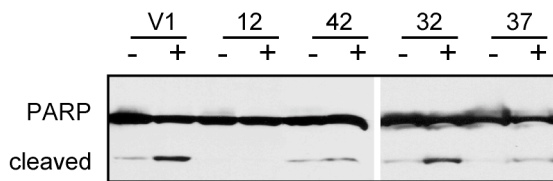
B



C

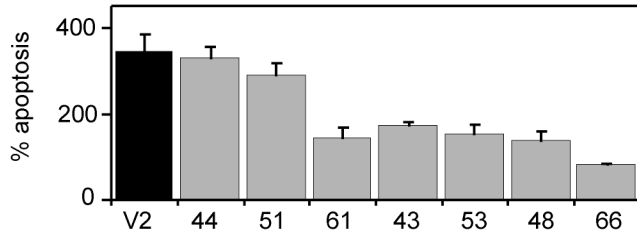


D

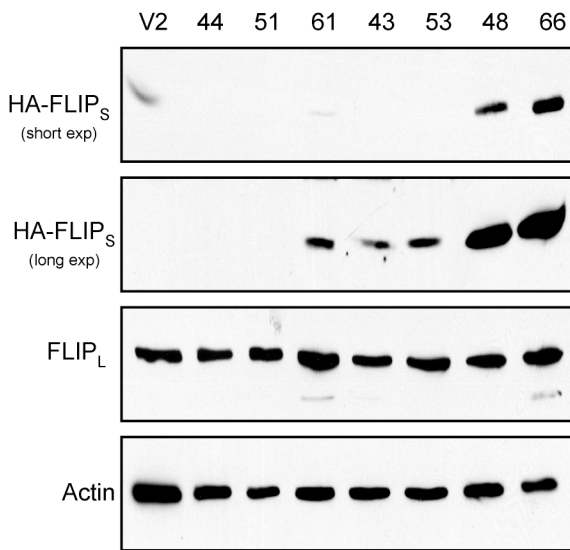


Nastiuk, et al, Figure 4

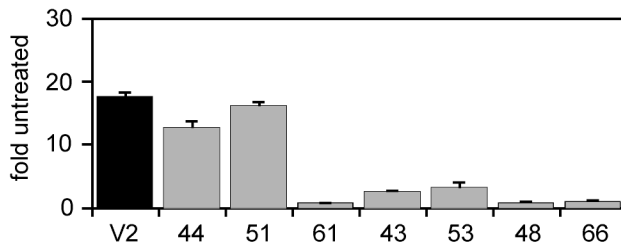
A



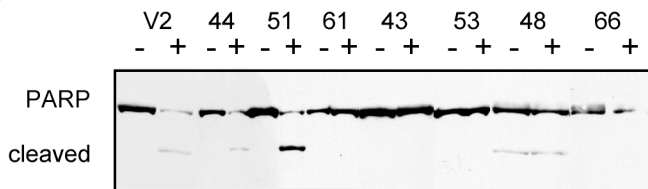
B



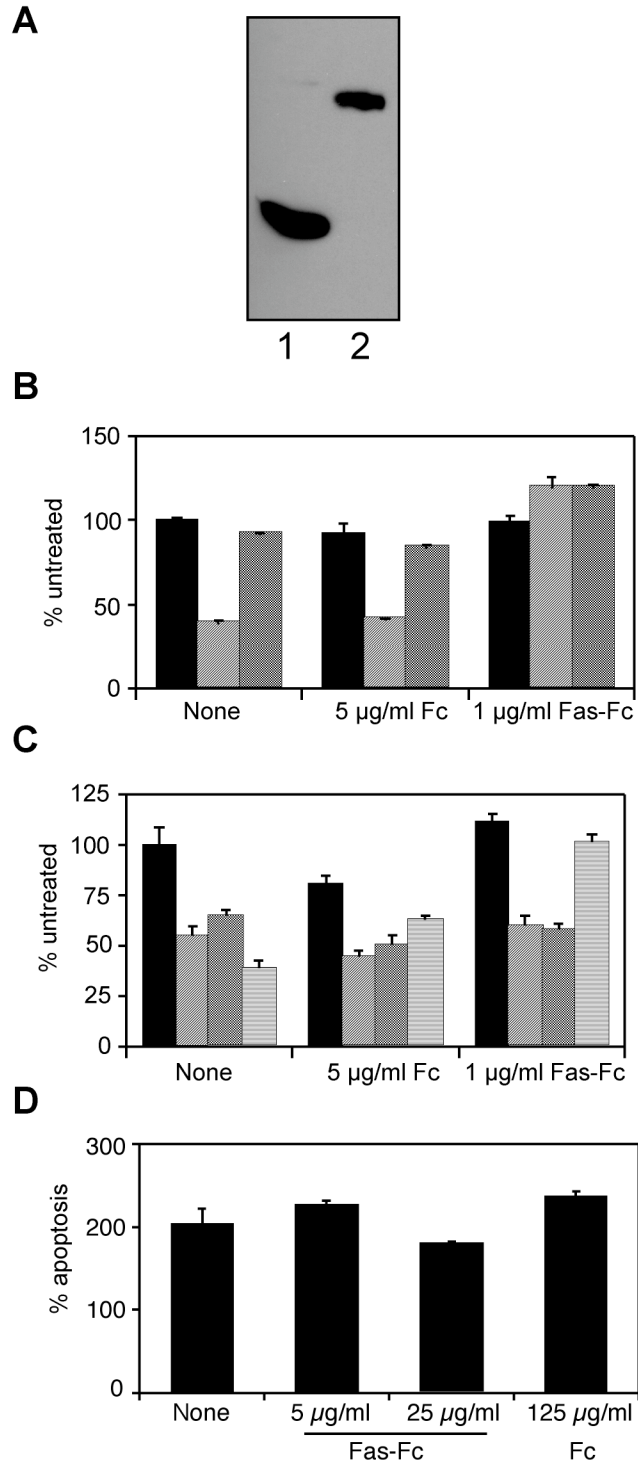
C



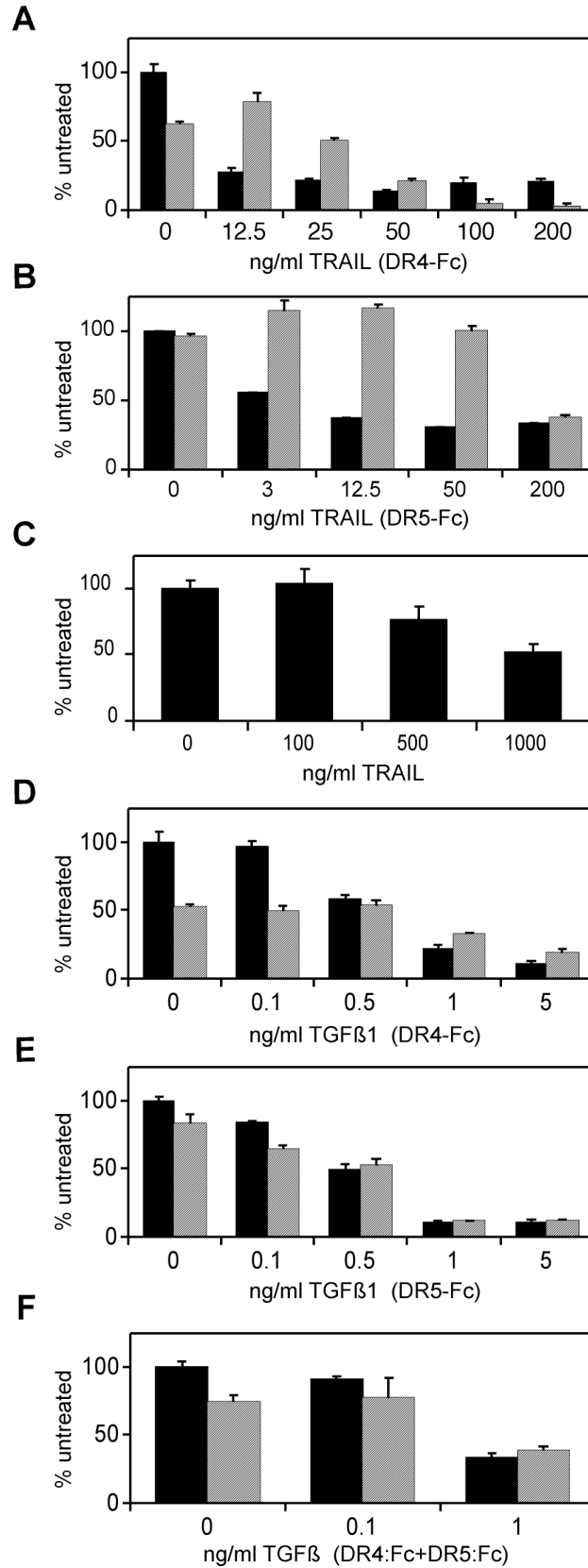
D



Nastiuk, et al., Figure 5

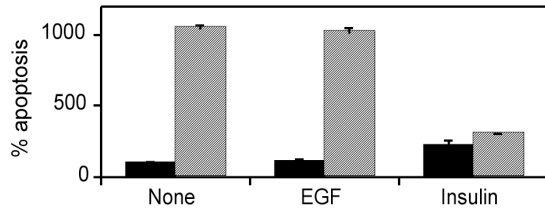


Nastiuk, et al., Figure 6

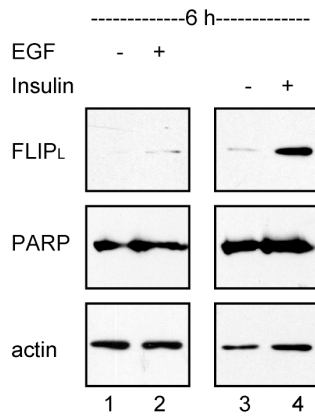


Nastiuk et al., Figure 7

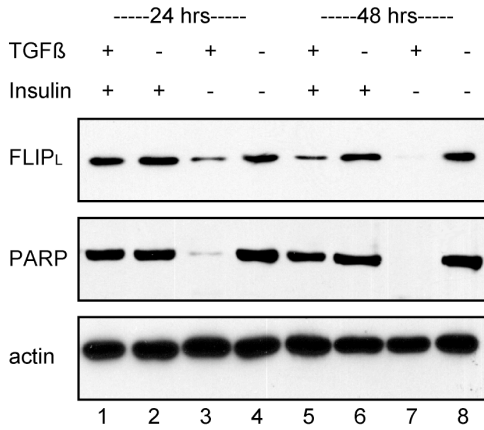
A



B



C



D

